

Spatiotemporal Variability of Longshore Sediment Transport on the Brazilian Coast

Thaisa Beloti Trombetta (✉ thaisabtrombetta@gmail.com)

Universidade Federal do Rio Grande - FURG

William Correa Marques

Universidade Federal do Rio Grande - FURG

Research Article

Keywords: Brazilian Coast, CERC, Kamphuis, Wavelets, Sediment Transport

Posted Date: September 1st, 2020

DOI: <https://doi.org/10.21203/rs.3.rs-68166/v1>

License:   This work is licensed under a Creative Commons Attribution 4.0 International License.

[Read Full License](#)

1 SPATIO-TEMPORAL VARIABILITY OF
2 LONGSHORE SEDIMENT TRANSPORT ON THE
3 BRAZILIAN COAST ☆

4 Trombetta, T. B.^{1,*}, Marques, W. C.^{1,*}

5 *Laboratório de Análise Numérica e Sistemas Dinâmicos (LANSD) - Instituto de*
6 *Matemática, Estatística e Física (IMEF) - Universidade Federal do Rio Grande (FURG) -*
7 *Brazil*

8 **Abstract**

The lack of planning and management regarding the transport of sediments along the coast can alter the existing equilibrium in coastal regions, causing or accelerating erosive processes and resulting in economic and environmental damage. Thus, it is important that the characteristics of the coastal drift be investigated, serving as source of information for future projects involving the coastal environment management. Within this context, the present work aims to identify the annual sediment transport averages along the Brazilian coast, the dominant direction of the coastal drift and its spatial variability. For this, a wind-generated wave modeling was considered, with 37 years of data (1979 to 2015), as well as four sediment transport formulations. For the spatiotemporal variability, the analysis of wavelets was applied, relating the effect of cycles of variability over the behavior of longshore sediment transport. The results showed that the largest annual volumes of sediment transport occurred in the northeastern Region of Brazil, reaching approximately $850\,000\text{ m}^3\text{ year}^{-1}$. On the other hand, the smallest transport averages occurred in the southern region, in the state of Santa Catarina, reaching the value of $13\,497\text{ m}^3\text{ year}^{-1}$. In the northeast region, annual and interannual cycles were more frequent and more energetic than in the southern Region, where short cycles presented similar importance to longer cycles, during 37 years of the study. However, in the overall context of the analysis, the long period cycles are more significant for longshore

*Corresponding author

Email address: thaisabtrombetta@gmail.com (Trombetta, T. B.)
Preprint submitted to Elsevier
Universidade Federal do Rio Grande (FURG), Itália Avenue, Km 8, Rio Grande - RS,
Brazil

sediment transport, since this is a long term process. In this way, the present article contributes with information on longshore sediment transport, highlighting the annual means and the dominant drift, and deals with important questions about the influence of cycles of variability in the study region, emphasizing the importance of longer period events for the control of sedimentary transport in the Brazilian coast.

- *Keywords:* Brazilian Coast, CERC, Kamphuis, Wavelets, Sediment
- 10 Transport.
-

11 **1. Introduction**

12 Sandy beaches present it own dynamic due to the mobility of sediments
13 transported by the constant effects of waves, coastal currents, tides and winds,
14 resulting in processes of beach accretion and/or erosion (Klein et al., 2006). The
15 movement of sediments transported along the coast, either by natural causes or
16 anthropogenic, can change the existing balance in certain environments, causing
17 or accelerating erosion processes and resulting in economic and environmental
18 damages (CERC, 1984).

19 The waves play a substantial role in coastal landscape, influencing the coastal
20 features, inputting morphological differences in space and time scales, according
21 to (Holthuijsen, 2007). In addition, the study of coastal dynamics involves the
22 evaluation of the distribution of wave energy, the patterns of sediment dispersion
23 and the balance of sediment along the coast (Silva et al., 2007).

24 The longshore sediment transport is a conditioning factor for the occurrence
25 of morphological changes in coastal environments. Therefore, prior knowledge
26 of the local wave climate and coastal sediment transport represents an essential
27 source of information for the design of projects, coastal management plans and
28 applications in erosion risk analysis.

29 Several studies were carried out at national and global level to analyze the
30 patterns of dispersal of the longshore sediment transport. For example, Giosan
31 et al. (1996) on the Black Sea coast, in Romania, Kumar et al. (2000) along the
32 coast of Kannirajapuram, India, and Oliveira et al. (2004) in the Portuguese
33 west coast. In all studies the results obtained improve the knowledge of the
34 variation of the longshore transport along the beach profile, its average annual
35 value, and a way to quantify other parameters that characterize the coastal zone
36 where the sediment transport induced by waves is significant.

37 Considering researches in Brazil, once there are hundreds of coastal areas
38 where the process of environmental change became very sharp and harmful, it is
39 important highlight Bittencourt et al. (2005), Moura and Morais (2011), Oliveira
40 et al. (2015) and Silva et al. (2016), which estimated the pattern of sediment

41 dispersion in different regions. Recently, [Trombetta et al. \(2020\)](#) studied the
42 potential of longshore sediment transport by the action of waves considering all
43 Brazilian coast, showing that there are many studies associated with this issue.

44 The space-time variability in sediment transport is able to predict the effects
45 of the passage of short and long-term phenomena, such as cold fronts, changes
46 in the seasons, El Niño events, for different regions. However, this analysis is
47 little studied, and has no applications along the Brazilian coast. Within this
48 perspective, the present work has as main objective to investigate the effect of
49 short and long period cycles (intra-seasonal, seasonal, annual and interannual
50 weekly) in the sediment transport along the entire Brazilian coast, considering
51 a period of 37 years.

52 *1.1. Study Area*

53 The study area involves all Brazilian coast, extending for approximately
54 9000 km, between 4° N, near Cabo Orange in Amapá state, and 34° S, at Arroio
55 Chuí in Rio Grande do Sul state (Figure 1). The Brazilian continental margin
56 has a substantial physic and environment diversity, being a challenge for the
57 coastal management. This diversity is characterized for heterogeneity in relation
58 to the coastal morphology and hydrodynamics components.

59 According to [Short and Klein \(2016\)](#), the long extension of the Brazilian
60 coast, climates variety and coastal processes requires that the littoral be divided
61 em different sectors, with the purposes to understand the impacts of these as-
62 pects on the coast and beach systems. In addition, [Tessler and Goya \(2005\)](#)
63 explained that Brazil has many climatic, oceanographer e geomorphological el-
64 ements that condition certain processes in different coastal segments.

65 In this paper, the longshore sediment transport will be presented in some
66 points of the study area, followed by the analysis of the spatiotemporal variabil-
67 ity throughout the Brazilian coast. Again, some places will be chosen to further
68 the discussion.

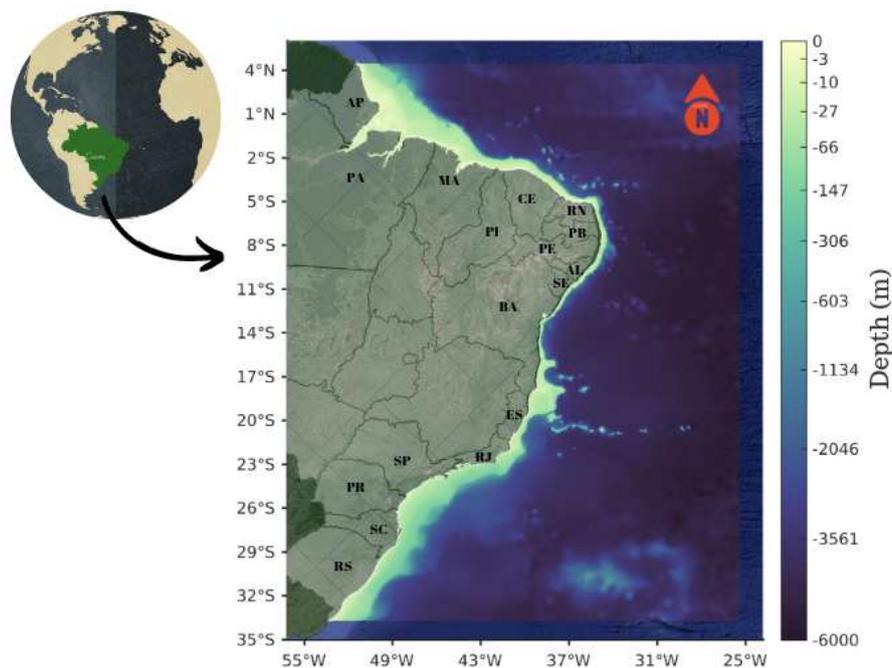


Figure 1: Representation of the study area, with bathymetric data and pointing coastal states - Amapá (AP), Pará (PA), Maranhão (MA), Piauí (PI), Ceará (CE), Rio Grande do Norte (RN), Paraíba (PB), Pernambuco (PE), Alagoas (AL), Sergipe (SE), Bahia (BA), Espírito Santo (ES), Rio de Janeiro (RJ), São Paulo (SP), Paraná (PR), Santa Catarina (SC) and Rio Grande do Sul (RS). The colorbar represents the depth in meters.

69 2. Methodology

70 This study involves the analysis of sediment transport throughout the Brazil-
 71 ian coast, considering mathematical formulas and numerical simulations. A
 72 third generation wave model was applied to simulate the sea state, for a pe-
 73 riod of 37 years (1979 to 2015). The numerical domain was represented by an
 74 unstructured mesh composed of 547 479 nodes, with a distance between 500 m
 75 on the coastline (region of interest in the study) and 55 km near the oceanic
 76 boundary, according to Figure 2.

77 The wave model TOMAWAC (TELEMAC-Based Operational Model Ad-
 78 dressing Wave Action Computation²) was used to simulate the sea state on the
 79 Brazilian coast. This model is maintained by the consortium open TELEMAC-

²www.opentelemac.org

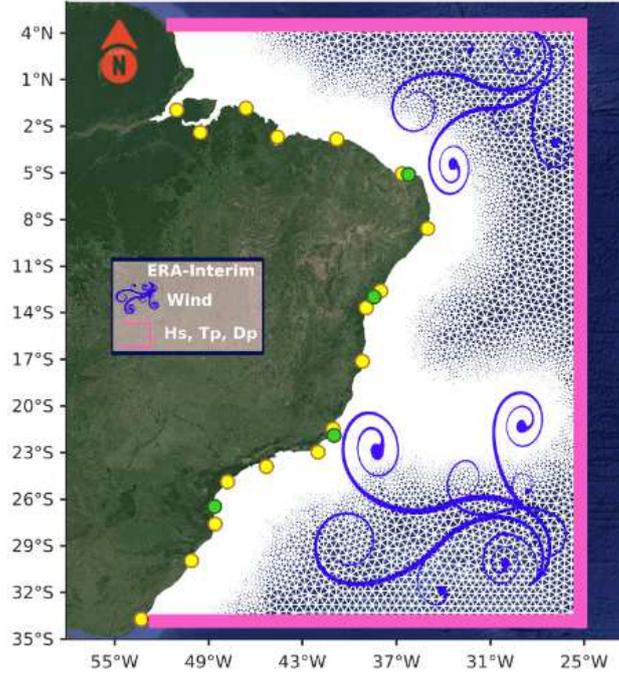


Figure 2: Figure of the computational domain with surface and boundary conditions. The points represent the areas used to analyze the spatial (in yellow) and temporal (in green) variability. The pink lines and the blue symbols represent wave and wind data, respectively.

80 MASCARET, and was developed by [Benoit et al. \(1996\)](#).

81 TOMAWAC is a spectral wave model that calculates the sea state by solv-
 82 ing the Wave Action Density Conservation Equation ([Hasselmann et al., 1988](#);
 83 [Holthuijsen et al., 1998](#)). As reported by [Awk \(2017\)](#), this wave model is able to
 84 calculate the changes in the wave energy spectrum generated by the wind and
 85 also the wave agitation for applications in the ocean and coastal domains.

86 In order to carry out the simulations, the surface of the TOMAWAC model
 87 has been forced with wind data, interpolated at all points of the numerical
 88 mesh (blue symbols in Figure 2). The oceanic contour was forced with signifi-
 89 cant height data (H_s), peak period (T_p) and average wave peak direction (D_p),
 90 inserted in mesh oceanic boundary (pink lines in Figure 2).

91 The wave and wind data of boundary conditions were obtained from the

92 ERA Interim Reanalysis Project³ from ECMWF (European Centre for Medium-
 93 Range Weather Forecasts), for the time period ranging from 1979 to 2015. The
 94 data used as initial and boundary conditions were interpolated and prescribed
 95 for each point of the finite element mesh, with a spatial resolution of 0.75° of
 96 latitude and longitude, and temporal resolution of 6h.

97 The longshore sediment transport was calculated using mathematical formu-
 98 las, which was proposed by the Coastal Engineering Research Center (CERC,
 99 1984) and by Kamphuis (1991). These methodologies are widely used for re-
 100 searches and presents coherent results when compared with *in situ* data.

101 Wave parameters, beach profiles and sedimentary characteristics were con-
 102 sidered in the calculations to estimate the sediment transport. In addition,
 103 in the CERC (1984) formula, there is an dimensionless coefficient (K) that di-
 104 rectly relates the longshore sediment transport with the waves energy flow (Lima
 105 et al., 2002). The value recommended by CERC (1984) for this coefficient is
 106 0.39, considering American beaches. In this way, for the expression becomes
 107 more reliable, other values of K were analyzed, considering the formulas pro-
 108 posed by Kamphuis et al. (1986) and Mil-Homens et al. (2013), according to
 109 Table 1.

Table 1: Mathematical formulas used in the calculation of the longshore sediment transport.	
CERC (1984)	$Q_v = 0.0625K\rho_a g^{0.5} H_{s,b}^{2.5} [\sin(2\alpha_b)] (\gamma_b)^{-0.5} (\rho_s - \rho_a)^{-1} (1-p)^{-1}$
<i>Recommended to American Beaches</i>	$K = 0.39$
<i>Kamphuis et al. (1986)</i>	$K = 0.022(\gamma_b H_{s,b})^{0.5} (D_{50})^{-0.5}$
<i>Mil-Homens et al. (2013)</i>	$K = [2237.7(H_{s,b})^{1.45} (L_0)^{-1.45} + 4.505]^{-1}$
Kamphuis (1991)	$Q_v = 6.4 \times 10^4 (H_{s,b})^2 (T_p)^{1.5} (m_b)^{0.75} (D_{50})^{-0.25} [\sin^{0.6}(2\alpha_b)]$

110 In these equations, K is the dimensionless coefficient, ρ_a is the sea water
 111 density (1025 kg m^{-3}), g is the acceleration of gravity (9.81 m s^{-2}), $H_{s,b}$ is the
 112 significant wave height at the breaker (m), α_b is the wave incidence angle at
 113 the breaker (°), γ_b is the breaker parameter (typically 0.78), ρ_s is the sediment

³www.ecmwf.int

114 density (typically 2650 kg m^{-3}), p is the sediment porosity (typically 0.4), D_{50}
 115 is the median particle diameter of sediments, L_0 is the wavelength (m), T_p is
 116 the wave peak period and m_b is the slope of the beach profile at the breaker.

117 The sedimentological data of the study region (Table 2) were obtained by
 118 the expeditions of the ReviZEE Program and prepared by the *Diretoria de*
 119 *Hidrografia e Navegação* - Brazil. The formulations proposed by CERC (1984)
 120 and Kamphuis (1991) consider only a sedimentary fraction, so the distribution
 121 of sediments throughout the study region has been simplified.

Table 2: Distribution of sedimentological data along the Brazilian coast based on the ReviZEE Program.

Sediment Fraction	D_{50} (mm)	Stretch
Muddy sand/Very fine sand	0.06	Cabo Orange (AP) to Parnaíba (PI)
Coarse sand	1	Parnaíba (PI) to Maceió (AL)
Medium sand	0.5	Maceió (AL) to Cabo Frio (RJ)
Muddy sand/Very fine sand	0.06	Cabo Frio (RJ) to Chuí (RS)

Amapá (AP), Piauí (PI), Alagoas (AL), Rio de Janeiro (RJ) and Rio Grande do Sul (RS).

122 The spatiotemporal variability of the longshore sediment transport was in-
 123 vestigated through the wavelet analysis, following the methodology proposed
 124 by Torrence and Compo (1998) and rectified by Liu et al. (2007) and Veeda
 125 et al. (2012). The spatial variability was analyzed for a transect (which con-
 126 nects the yellow dots in Figure 2), towards the usage of the wavelet analysis.
 127 In the two-dimensional analysis, a DOG wavelet (known as Mexican Hat) was
 128 considered.

129 At first, all the formulas used in the calculation of sediment transport were
 130 investigated, resulting in similar patterns in relation to spatial variability's for
 131 cycles between 100 and 1000 days. Thus, for this article, the formulation of
 132 CERC (1984), with the parameter K calibrated by Kamphuis et al. (1986),
 133 was chosen to compose this analysis, since it represented one of the formulas
 134 considered most suitable for the calculation of sedimentary transport in several
 135 sectors of the Brazilian coast.

136 The wavelet method also allowed the analysis of the temporal variability

137 of longshore sediment transport along the Brazilian coast. For this analysis,
138 four points were selected located in Galinhos - Rio Grande do Norte, Salvador
139 - Bahia, Praia do Açú - Rio de Janeiro and Balneário Barra do Sul - Santa
140 Catarina, which are indicated by the green dots in Figure 2. For each point,
141 the sediment transport formula considered more adequate was used with the
142 application of one-dimensional DOG wavelet.

143 2.1. Validation

144 The validation of the numerical model TOMAWAC was realized comparing
145 the main wave characteristics of the Brazilian continental shelf with measured
146 data by four buoys from the *Programa Nacional de Boias - Brazil* (PNBOIA⁴).
147 These buoys are located in Recife - Pernambuco, Cabo Frio - Rio de Janeiro,
148 Santos - São Paulo and Rio Grande - Rio Grande do Sul, at 200 m depth,
149 covering the period from 2010 until 2015.

150 Validation is important to properly reproduce the main wave characteristics
151 of the Brazilian continental shelf in the model. Thus, the significant height (H_s)
152 and the peak period (T_p) of the waves were analyzed through Statistical metrics,
153 as show in Table 3.

Table 3: Statistical metrics calculated by comparing modeled data and measured data.

	RECIFE - PE		CABO FRIO - RJ		SANTOS - SP		RIO GRANDE - RS	
	Modeled	Measured	Modeled	Measured	Modeled	Measured	Modeled	Measured
HS (m)	1.6476	1.6054	1.5863	1.2322	1.6264	1.9586	1.6512	1.9979
ER (m)		0.0262		0.2874		0.1696		0.1735
MAE (m)		0.0421		0.3541		0.3322		0.3467
RMSE (m)		0.2902		0.7305		0.5977		0.7482
Bias (m)		-0.0421		-0.3541		0.3322		0.3467
Tp (s)	8.5713	8.5713	8.4079	10.5817	8.4096	9.6381	8.6140	8.9654
ER (s)		0.0174		0.2054		0.1274		0.0391
MAE (s)		0.1520		2.1738		1.2285		0.3514
RMSE (s)		2.2249		3.5947		2.7904		2.4992
Bias (s)		0.1520		2.1738		1.2285		0.3514

Pernambuco (PE), Rio de Janeiro (RJ), São Paulo (SP) and Rio Grande do Sul (RS).
Relative Error (ER), Mean Absolute Error (MAE) and Root Mean Square Error (RMSE).

154 The comparison of the statistics showed a good correlation between the
155 modeled data by TOMAWAC and measured data by PNBOIA, as shown by the
156 similarity in the values of H_s and T_p in all sites. Besides that, all statistical

⁴<http://www.goosbrasil.org/pnboia>

157 metrics resulted close to zero, highlighting the Relative Error (ER) and the
 158 Mean Absolute Error (MAE) presented in Recife, with the lowest values.

159 In addition, the Root Mean Square Error (RMSE) resulted close to zero for
 160 H_s in all sites, representing a low magnitude of the error. This metric resulted
 161 near to 2.5 for the T_p , but is important explain that this parameter is less
 162 important than H_s in the sediment transport formulas considered in this study.

163 The Bias values were considered to indicate whether the model is overesti-
 164 mating (positive values) or underestimating (negative values) the *in situ* data.
 165 As shown, the values of H_s in TOMAWAC model are underestimated for Cabo
 166 Frio and Recife, unlike the other sites.

167 In this way, it was possible to verify a good correlation between the modeled
 168 and measured data, verifying the reliability of TOMAWAC model for the pur-
 169 poses of this study. Besides, TOMAWAC model was also validated along the
 170 Brazilian coast in the studies of Kirinus et al. (2018), Guimarães et al. (2019)
 171 and Trombetta et al. (2020).

172 The verification of the longshore sediment transport was carried out by com-
 173 paring the annual rates calculated with the formulations presented previously
 174 and the results of Brazilian studies related to the theme. Thus, the study area
 175 was divided into different sectors and all formulas were tested, according to
 176 Table 4.

Table 4: Longshore sediment transport rates in $\text{m}^3 \text{year}^{-1}$. Negative values indicate that the liquid transport direction is towards South.

Localização	CERC (1984)			Kamphuis (1991)	Previous Studies
	0,39	Kamphuis et al. (1986)	Mil-Homens et al. (2003)		
Galinhos - RN	322 640	14 549	86 275	52 690	185 839
Natal - RN	846 680	44 473	134 430	160 560	250 000
Aracaju - SE	- 1 392 600	- 101 320	- 208 830	- 500 590	- 355 600
Salvador - BA	- 101 430	- 9 397	- 45 048	- 166 430	- 194 500
Linhares - ES	- 2 123 900	- 162 390	- 364 410	- 107 610	161 000
Vila Velha - ES	- 2 709 700	- 218 040	- 465 840	- 1 378 900	- 205 588
Itapemirim - ES	1 049 700	66 431	215 650	295 105	69 313
Barra do Açú - RJ	2 159 600	165 480	316 010	289 090	182 500
Cibratel - SP	- 1 654 000	- 356 760	-296 940	- 521 410	- 400 000
Matinhos - PR	625 580	142 240	115 010	118 500	188 496
Baln. Barra do Sul - SC	1 767 500	402 970	314 490	1 109 300	459 900

RN - Rio Grande do Norte; SE - Sergipe; BA - Bahia; ES - Espírito Santo;
 RJ - Rio de Janeiro; SP - São Paulo; PR - Paraná; SC - Santa Catarina.

177 The first site tested was in Galinhos - Rio Grande do Norte, where the

178 longshore sediment transport rates calculated with the four formulations were
179 compared with the study of [Marcelino et al. \(2018\)](#). These authors found
180 $185\,839\text{ m}^3\text{ year}^{-1}$ for the analyzed area, with a predominant direction west-
181 ward.

182 The results of the formulas considered in the present study indicated the
183 same predominant direction, and the formulation proposed by [CERC \(1984\)](#),
184 with the parameter K by [Mil-Homens et al. \(2013\)](#), was the one that best ap-
185 proached the rate found by [Marcelino et al. \(2018\)](#), resulting in $86\,275\text{ m}^3\text{ year}^{-1}$.
186 In this way, this formulation was chosen to represent the sectors close to Gal-
187 inhos, more precisely between Parnaíba - Piauí and Touros - Rio Grande do
188 Norte.

189 Another site tested was in Natal - Rio Grande do Norte, where the study of
190 [Araújo \(2015\)](#) was considered in the analysis. The results of longshore sediment
191 transport calculated for these authors showed the predominant direction north-
192 ward, with a rate of $250\,000\text{ m}^3\text{ year}^{-1}$. In the present study, the predominant
193 direction also resulted northward for the four formulas, and the methodology
194 proposed by [Kamphuis \(1991\)](#) was the most similar to the study of [Araújo](#)
195 [\(2015\)](#).

196 At Aracajú - Sergipe, the average sediment transport rate of $500\,590\text{ m}^3\text{ year}^{-1}$
197 was obtained by [Kamphuis \(1991\)](#) formulation, with predominant direction to-
198 ward the south. This site was compared with the study results of [Bittencourt](#)
199 [et al. \(2005\)](#), which found rates of approximately $355\,600\text{ m}^3\text{ year}^{-1}$ with south-
200 ward direction, validating the results of the present study.

201 [Bittencourt et al. \(2005\)](#) also found rates of $194\,500\text{ m}^3\text{ year}^{-1}$ with domi-
202 nant direction southward, in Salvador - Bahia, which is similar to the rate of
203 $166\,430\text{ m}^3\text{ year}^{-1}$ calculated in the present work using the [Kamphuis \(1991\)](#) for-
204 mulation. Thus, this formula was considered to represent the sectors between
205 Carnaubinha - Rio Grande do Norte and Canavieiras - Bahia.

206 The last sector defined involves Linhares - Espírito Santo, where [Oliveira](#)
207 [et al. \(2015\)](#) found an average of $161\,000\text{ m}^3\text{ year}^{-1}$, which is similar to the

208 result calculated using the [CERC \(1984\)](#) formulation, with the parameter K by
209 [Kamphuis et al. \(1986\)](#). The result reached $162\,390\text{ m}^3\text{ year}^{-1}$, and the transport
210 was northward in both studies, showing that the data is validated.

211 In Vila Velha and Itapemirim beaches, also in Espírito Santo, [Contti Netto](#)
212 [\(2013\)](#) found transport rates similar to those obtained in the present study
213 by applying the [CERC \(1984\)](#) formulation, with K calibrated by [Kamphuis](#)
214 [et al. \(1986\)](#). The author found values of $205\,588\text{ m}^3\text{ year}^{-1}$ directed southward
215 and $69\,313\text{ m}^3\text{ year}^{-1}$ directed northward, respectively. The rates are similar
216 to the rate calculated by the present study, respectively $218\,040\text{ m}^3\text{ year}^{-1}$ and
217 $66\,431\text{ m}^3\text{ year}^{-1}$.

218 In the southeastern region, in Barra do Açu - Rio de Janeiro state, the
219 formulation of [CERC \(1984\)](#), with K calibrated by [Kamphuis et al. \(1986\)](#),
220 was the one that better approximated the results obtained by [Bastos and Silva](#)
221 [\(2000\)](#). The values calculated in both studies reaches $165\,480\text{ m}^3\text{ year}^{-1}$ and
222 $182\,500\text{ m}^3\text{ year}^{-1}$, respectively, with predominant direction northward.

223 In São Paulo state, the transport rate was validated at Cibratel beach based
224 on the proximity of the results given by the [CERC \(1984\)](#) formulation, with
225 K calibrated by [Kamphuis et al. \(1986\)](#) and the outcomes obtained by [Araújo](#)
226 [and Alfredini \(2001\)](#). The average transport was similar in the studies, reaching
227 $356\,760\text{ m}^3\text{ year}^{-1}$ and $400\,000\text{ m}^3\text{ year}^{-1}$, respectively, and dominant direction
228 toward the south, which validates the results.

229 At Matinhos beach - Paraná, [Wosiacki and Gobbi \(2012\)](#) found an average of
230 $188\,500\text{ m}^3\text{ year}^{-1}$, with a predominant direction toward the north. This result
231 is similar to the transport calculated using the [CERC \(1984\)](#) formula, with K
232 calibrated by [Kamphuis et al. \(1986\)](#), which gives a rate of $142\,240\text{ m}^3\text{ year}^{-1}$,
233 also northward.

234 In the Southern region, [Castilhos and Gré \(2006\)](#) found a transport rate
235 of $459\,900\text{ m}^3\text{ year}^{-1}$ at Balneário Barra do Sul - Santa Catarina. This rate is
236 similar to the one calculated using the [CERC \(1984\)](#) formula, with K calibrated
237 by [Kamphuis et al. \(1986\)](#), which resulted in $402\,970\text{ m}^3\text{ year}^{-1}$. Moreover, the

238 transport direction toward north validates the analyzed site. In this way, this
 239 formulation was chosen to represent the sectors between Belmonte, in Bahia,
 240 and Meia Praia, in Santa Catarina.

241 The annual averages calculated for the longshore sediment transport were
 242 orders of magnitude similar to existing studies in the literature. Hence, for
 243 the present article, the rates were calculated in eleven sites along the Brazilian
 244 coast, considering a specific method for each sector, according to Table 5.

Table 5: Definition of the methodology used in each stretch along the Brazilian coast in comparison with past studies.

Stretch	Methodology
Parnaíba (PI) to Touros (RN)	CERC (1984) - K calibrated by Mil-Homens et al. (2013)
Carnaubinha (RN) to Canavieiras (BA)	Kamphuis (1991)
Belmonte (BA) to Meia Praia (SC)	CERC (1984) - K calibrated by Kamphuis et al. (1986)
Piauí (PI), Rio Grande do Norte (RN), Bahia (BA) and Santa Catarina (SC)	

245 In addition, as expected, the dominant direction of littoral drift also had a
 246 good agreement within the analyzes, since it is highly influenced by the waves
 247 climate already validated. In this way, the formulas considered for the calcu-
 248 lation of the longshore sediment transport proved to be adequate in different
 249 sectors of the Brazilian coast, with the exception of the CERC (1984) formula-
 250 tion, with the K equal to 0.39, which overestimated the results in all situations.

251 A fraction of the South region and in the North region of Brazil were not
 252 considered in the calculation of the longshore sediment transport. This occurs
 253 due to the possibility of these sectors being influenced by the boundary condi-
 254 tions imposed into the numerical domain of TOMAWAC Model, which possibly
 255 caused variations in the results. In addition, the southern region has been sub-
 256 ject of many studies, for example Calliari and Klein (1993), Barletta (2000),
 257 Lima et al. (2002), Siegle and Asp (2007), Martinho et al. (2009) and Silva
 258 et al. (2016).

259 **3. Results and Discussions**

260 This section presents the results obtained from the analysis of the waves
261 generated by wind behaviour, over 37 years (between 1979 and 2015). These
262 results were applied in the calculation of the longshore sediment transport and,
263 consecutively, an analysis of the spatiotemporal variability was performed.

264 Results obtained for the averages of significant height (H_s , in meters), peak
265 period (T_p , in seconds) and direction of incidence of waves (M_d , in degrees) are
266 derived from a simulation of waves generated by the wind. Figure 3 shows a
267 schematic representation of the mean values obtained over all years simulated.

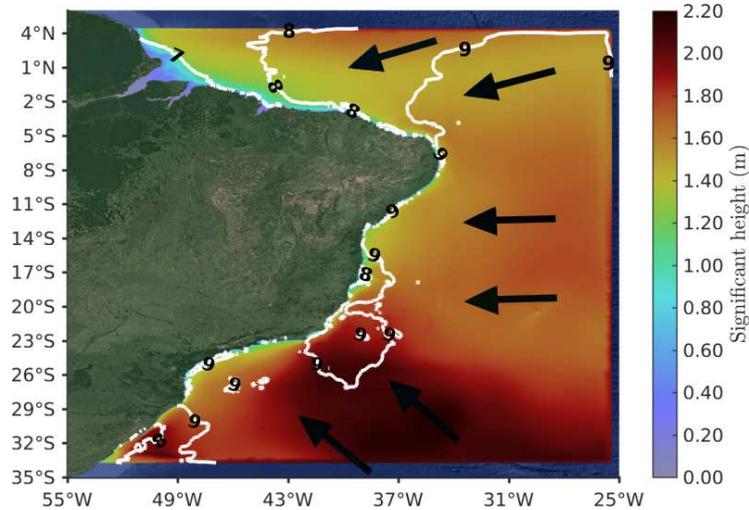


Figure 3: Results of the Brazilian Continental Shelf, overlapping image by Google Maps, Landsat/Copernicus, 2018. Frame shows H_s (m) in the surface, T_p (s) in the isolines and M_d in the arrows.

268 The results show that the distribution of the significant wave height over the
269 entire Brazilian continental shelf is highly variable, with considerable variability
270 between the northern and southern regions. The highest averages occurred in
271 the South region, with values close to 1.2 m in the coastal zone of Rio Grande
272 do Sul and Santa Catarina, decreasing to 0.8 m in Paraná.

273 In the Southeastern region, the averages remained at approximately 0.8 m
274 in the coastal zone. An exception occurs in Cabo Frio and Cabo de São Thomé,
275 both in Rio de Janeiro, where maximum values of 1.8 m are observed in the

276 offshore, once reflexive beaches characterize the region.

277 Finally, the north and northeast regions of Brazil presented smaller mean
278 significant wave height when compared to the South. The values reached ap-
279 proximately 0.6 m in the coastal zone, and in the adjacencies of the Amazon
280 River mouth presented even smaller significant wave height.

281 For the M_d , from the state of Amapá to Ceará, in the Northern Region,
282 prevail the waves incidents of East and Northeast. The atmospheric system of
283 the Brazilian equatorial region is related to the Intertropical Convergence Zone,
284 which generates the trade winds from Northeast and Southeast that converge
285 in the region (McGregor and Nieuwolt, 1998).

286 In the sector between the Rio Grande do Norte and the Espírito Santo, the
287 predominant direction of incidence is East, with variations in specific regions of
288 this passage. Dominguez (2009) showed that the main atmospheric circulation
289 of this sector is determined by the South Atlantic Subtropical Anticyclone, with
290 small variability linked to the seasonal cycles.

291 Finally, between Rio de Janeiro and Rio Grande do Sul, the waves come
292 from East and Southeast. The atmospheric circulation pattern varies according
293 to seasonal oscillations and the intensity and position of the South Atlantic
294 Subtropical Anticyclone, according to Oliveira (2002). The passage of cold
295 fronts over the region can interrupt this behavior, turning the wind direction to
296 the Southern quadrant. These results showed a high discrepancy in the averages
297 of H_s and M_d , in all the Brazilian continental shelf, mainly in relation to the
298 northern and southern regions.

299 On the other hand, the wave T_p showed values similar throughout the area
300 analyzed, varying between 7 and 9 s. The most frequent values are near 9 s,
301 which is typical of swell waves generated by distant storms. The waves with
302 shorter periods are classified as seas, and usually, they are caused by the effect
303 of the local wind blowing on the sea surface.

304 The results presented in this section are in agreement with previous studies
305 carried out by Pianca et al. (2010); Espindola and Araújo (2017); Guimarães

306 [et al. \(2019\)](#) and [Trombetta et al. \(2020\)](#). These authors analyzed the wave
 307 climate along the Brazilian coast from a combined approach, using data analysis
 308 and numerical modeling.

309 3.1. Longshore Sediment Transport Rates

310 Regarding the longshore sediment transport rates, some sites in the Brazilian
 311 coast were chosen to the calculation, considering a specific methodology for each
 312 region, with the corresponding diameter of sediments, as shown in Tables 6, 7
 313 and 8. It is valid to emphasize that due to the proximity of the regions north
 314 and south of Brazil to the boundary conditions of the numerical model, these
 315 regions were excluded to the analysis of this study.

Table 6: Representation of longshore sediment transport rates (LST) in $\text{m}^3 \text{year}^{-1}$, considering D_{50} equal to 1 mm.

Diameter	CERC (1984)	LST ($\text{m}^3 \text{year}^{-1}$)	Kamphuis (1991)	LST ($\text{m}^3 \text{year}^{-1}$)
	Coefficient K calibrated by Mil-Homens et al. (2013)			
1 mm	Parnaíba - PI	48 200	Carnaubinha - RN	39 470
	Praia de Atalaia - PI	133 800	Maxaranguape - RN	86 014
	Praia de Maramar - PI	66 054	Ceará-Mirim - RN	102 290
	Praia de Barra Grande - PI	120 310	Natal - RN	160 560
	Barroquinha - CE	150 690	Parnamirim - RN	126 630
	Camocim - CE	89 247	Tibau do Sul - RN	261 560
	Acaraú - CE	43 188	Barra de Camaratuba - PB	138 860
	Itarema - CE	110 440	Balneário Lucena - PB	37 123
	Itapipoca - CE	88 403	Cabedelo - PB	154 000
	Paracuru - CE	397 610	Costa do Sol - PB	259 170
	Caucaia - CE	52 516	Praia do Amor - PB	124 650
	Fortaleza - CE	442 670	Pitimbu - PB	172 440
	Beberibe - CE	225 630	Pontas de Pedra - PE	215 650
	Aracati - CE	277 690	Olinda - PE	418 600
	Icapuí - CE	57 962	Pina - PE	765 810
	Porto do Mangue - RN	52 412	Sirinhaém - PE	325 960
	Galinhos - RN	86 275	Maragogi - AL	708 720
	Touros - RN	387 750	Barra de Santo Antônio - AL	342 330

Ceará (CE), Rio Grande do Norte (RN), Paraíba (PB), Pernambuco (PE) and Alagoas (AL).

316 The mean liquid sediment transport behavior, over the 37 years simulated,
 317 can be explained due the wave climate, which is the main variable in the short
 318 and medium term coastal processes. As demonstrated in the Table 6, the for-
 319 mula of [CERC \(1984\)](#), with the coefficient K calibrated by [Mil-Homens et al.](#)
 320 (2013), was the most suitable for the calculation of the longshore sediment
 321 transport between Parnaíba (Piauí) and Touros (Rio Grande do Norte), where
 322 it was considered an average diameter of 1 mm, corresponding to a sedimentary
 323 fraction of coarse sand.

324 In this sector of the Northeast Region of Brazil, the waves are generated by
325 the action of the trade winds (Tessler and Goya, 2005), resulting in the whole
326 movement (atmospheric or oceanic) directed from East to West (Muehe, 1998).
327 Thus, in this coastal segment, the drift has dominant sense to the West, as
328 indicated by the positive averages in Table 6.

329 Trombetta et al. (2020) corroborates with these results, showing values of
330 angles of incidence greater than 0° in this region, indicating that the waves are
331 derived from East and Northeast and, therefore, at all points, the dominant
332 drift is directed to the West. In addition, the same results are indicated in the
333 Figure 3, where the arrows demonstrate the dominant direction of incidence
334 of waves. The average annual sediment transport do not present large varia-
335 tions between Parnaíba and Touros, reaching maximum of $442\,000\text{ m}^3\text{ year}^{-1}$ in
336 Fortaleza, Ceará, and at least $43\,188\text{ m}^3\text{ year}^{-1}$ in Acaraú, in the same state.

337 Analyzing the other points of the Table 6, it is possible to observe that
338 between Carnaubinha - Rio Grande do Norte and Barra de Santo Antônio -
339 Alagoas, the formulation of Kamphuis (1991) was defined as the most appro-
340 priate for the estimation of the longshore sediment transport. In addition, for
341 this segment, the average diameter of sediments remained equal to 1 mm, cor-
342 responding to a coarse sand.

343 In the sector that involves the coast of Alagoas and Rio Grande do Norte,
344 the study of Trombetta et al. (2020) demonstrated that the incidence angles
345 are smaller than 0° , indicating that these come from Southeast and, therefore,
346 becoming the dominant drift to the North. The studies of Bittencourt et al.
347 (2005); Araújo (2015) and Gurgel (2017) corroborate these results, as well as
348 Tessler and Goya (2005) that point out that in this region receives only waves
349 generated from the Trade winds, indicating a transport resulting Northwards.

350 Regarding the average rates calculated for the longshore sediment transport,
351 it is observed a high diversity among the values, highlighting the greatest aver-
352 ages that occurred in Pina - Pernambuco and in Maragogi - Alagoas, reaching
353 $765\,810\text{ m}^3\text{ year}^{-1}$ and $708\,720\text{ m}^3\text{ year}^{-1}$, respectively. On the other hand, in

354 the sector further north there was a significant decrease of mean transported, re-
 355 sulting in 37 123 m³ year⁻¹ in Balneário Lucena - Paraíba, and 39 470 m³ year⁻¹
 356 in Carnaubinha - Rio Grande do Norte.

357 Table 7 presents the stretch between Maceió - Alagoas and Farol de São
 358 Thomé - Rio de Janeiro, where was considered the sediment fraction equal to
 359 0.5 mm, corresponding to medium sand. In the first sector, the formulation of
 360 Kamphuis (1991) proved to be the most appropriate, while in the second, the
 361 formulation of the CERC (1984), with the coefficient K calibrated by Kamphuis
 362 et al. (1986), had a more satisfactory result.

Table 7: Representation of longshore sediment transport rates (LST) in m³ year⁻¹, considering D_{50} equal to 0.5 mm.

Diameter	Kamphuis (1991)	LST (m ³ year ⁻¹)	CERC (1984)	
			Coefficient K calibrated by Kamphuis et al. (1986)	
				LST (m ³ year ⁻¹)
0.5 mm	Maceió - AL	-769 200	Belmonte - BA	127 780
	Jequiá da Praia - AL	-844 320	Santa Cruz - BA	121 150
	Feliz Deserto - AL	501 200	Trancoso - BA	142 110
	Piaçabuçu - AL	-450 320	Prado - BA	-61 034
	Pacatuba - SE	159 760	Alcobaça - BA	-31 069
	Barra dos Coqueiros - SE	-269 940	Mucurí - BA	-22 577
	Aracaju - SE	-500 590	São Mateus - ES	132 590
	Itaporanga d'Ajuda - SE	-262 610	Linhares - ES	162 390
	Jandaíra - BA	-133 280	Comboios - ES	-29 853
	Conde - BA	-382 930	Praia Formosa - ES	-169 030
	Entre Rios - BA	-672 790	Vila Velha - ES	-218 040
	Salvador - BA	-166 430	Nova Guarapari - ES	-154 500
	Valença - BA	-148 870	Itapemirim - ES	66 431
	Maraú - BA	604 100	Alto Lagoa Funda - ES	-82 975
	Itacaré - BA	648 340	São Francisco de Itabapoana - RJ	-71 836
	Ilhéus - BA	646 810	Atafona - RJ	-76 607
	Una - BA	293 640	Praia do Açú - RJ	165 480
	Canavieiras - BA	-54 035	Farol de São Thomé - RJ	122 460

Alagoas (AL), Sergipe (SE), Bahia (BA), Espírito Santo (ES) and Rio de Janeiro (RJ).

363 In these coastal sectors it is observed that the drift varies towards South and
 364 North on several points, due to the predominant incidence of the East waves,
 365 according to the Figure 3. This occurs because the wave climate in this region is
 366 maintained by the winds generated by the South Atlantic Anticyclone, according
 367 to Tessler and Goya (2005), with waves coming from the East, Northeast and
 368 Southeast. This behavior is also demonstrated in Trombetta et al. (2020), since
 369 variations in the direction of incidence of waves, interfering with the dominant
 370 pattern of littoral drift.

371 In the northern sector of Bahia, the drift is directed, in the majority of the

372 points analyzed, towards South, agreeing with the study of [Bittencourt et al.](#)
373 [\(2002, 2008\)](#). While between Maraú and Trancoso, within the same state, the
374 transport has dominant direction towards North ([Bittencourt et al., 2000, 2008](#)),
375 with the exception of Canavieiras.

376 In the south of Bahia, the drift return its direction pattern Southwards.
377 The patterns of sediment dispersion along the coast of Bahia vary according the
378 general orientation of the coastline and the system of atmospheric circulation,
379 therefore, this inversion occurs in the littoral drift along throughout the whole
380 state.

381 In the coastal segment between the state of Espírito Santo and the Farol de
382 São Thomé, the more effective waves for sediment transport are generated by the
383 winds of Northeast and East quadrants ([Tessler and Goya, 2005](#)), explaining the
384 directed drift, in most cases, towards South. In Linhares, the fact that the drift
385 outcome is towards North is in agreement with the study of [Oliveira et al. \(2015\)](#),
386 which demonstrated that the sediments provided by Rio Doce are transported
387 preferentially to North due to the action of the waves.

388 For the Rio de Janeiro littoral, the study of ([Bastos and Silva, 2000](#)) demon-
389 strated the occurrence of convergence in the littoral drift between Atafona and
390 the Praia do Açú, among with other authors ([Cassar and Neves, 1993](#); [Bastos](#)
391 [and Silva, 2000](#); [Machado et al., 2018](#)) that stated that the dominant direction
392 of sediment transport in the vicinity of the Cabo de São Thomé is Northward.
393 Thus, these studies are in agreement with the results presented in Table 7.

394 The calculated averages on the stretch between Maceió and Canavieiras pre-
395 sented the greatest values of longshore sediment transport in relation to any
396 other points analyzed on the Brazilian coast, reaching $844\,320\text{ m}^3\text{ year}^{-1}$ in Je-
397 quiá da Praia - Alagoas and $769\,200\text{ m}^3\text{ year}^{-1}$, in the neighbor city, Maceió.
398 The lower average occurred in Bahia State, at Canavieiras, reaching values of
399 $54\,035\text{ m}^3\text{ year}^{-1}$.

400 Among Belmonte and Farol de São Thomé, the rates of average sediment
401 transport resulted not too considerable, reaching a maximums of $218\,040\text{ m}^3\text{ year}^{-1}$

402 in Vila Velha - Espírito Santo. In Bahia, the values were quite discrepant, rang-
 403 ing from $142\,110\text{ m}^3\text{ year}^{-1}$ in Trancoso towards $22\,577\text{ m}^3\text{ year}^{-1}$ on Mucuri. In
 404 Espírito Santo the variations were also high, $218\,040\text{ m}^3\text{ year}^{-1}$ in Vila Velha un-
 405 til $29\,853\text{ m}^3\text{ year}^{-1}$ in Comboios. Rio de Janeiro, for instance, kept the averages
 406 on the order of $100\,000\text{ m}^3\text{ year}^{-1}$.

407 Moving southwards, in the Table 8, which presents the stretch among Saquarema
 408 - Rio de Janeiro and Meia Praia - Santa Catarina, the CERC (1984) formula,
 409 with the K coefficient calibrated by Kamphuis et al. (1986), was the best fit.
 410 For this segment, it was considered an average grain diameter of 0.06 mm, cor-
 411 responding to a sedimentary fraction of muddy sand/very fine sand.

Table 8: Representation of longshore sediment transport rates (LST) in $\text{m}^3\text{ year}^{-1}$, considering D_{50} equal to 0.06 mm.

Diameter	CERC (1984)	LST ($\text{m}^3\text{ year}^{-1}$)
	Coefficient K calibrated by Kamphuis et al. (1986)	
0.06 mm	Saquarema – RJ	690 670
	Barra da Tijuca – RJ	625 670
	Praia de Maresias – SP	153 390
	Cibratel – SP	- 356 760
	Iguape – SP	320 430
	Ilha Comprida – SP	24 067
	Guaraqueçaba – PR	237 710
	Matinhos – PR	142 240
	Itapoá – SC	56 895
	Balneário Barra do Sul – SC	402 970
	Balneário Piçarras – SC	-317 580
	Balneário Camboriú – SC	-172 650
	Meia Praia – SC	-13 497

Rio de Janeiro (RJ), São Paulo (S), Paraná (PR) and Santa Catarina (SC).

412 From the Cabo Frio region to southern Brazil, Pianca et al. (2010) stated
 413 that, overall, the waves generated by high South Atlantic storms are the most
 414 frequent, being the most energetic originated from the South and Southeast,
 415 which makes the dominant pattern of littoral drift towards Northeast. Figure 3
 416 demonstrated that the main direction of waves are from Southeast, thus agreeing
 417 with the results.

418 In the São Paulo coast, in Cibratel, it is observed that the transport has

419 dominant pattern for Southwest, in accordance with the study of [Araújo and](#)
420 [Alfredini \(2001\)](#). This exception occurs due to the change in the alignment of
421 the coast, along to the possible temporal predominance of the Atlantic Tropical
422 Anticyclone (source of waves of Northeast and East). However, it is valid to
423 emphasize that, in normal conditions where mobile Polar Anticyclones predom-
424 inate, the waves are coming from the South and Southeast directions, changing
425 the drift towards Northeast.

426 For the states of Paraná and Santa Catarina, some authors ([Gobbi, 1997](#);
427 [Veiga et al., 2004](#); [Castilhos and Gré, 2006](#); [Thoaldo, 2011](#); [Abreu, 2011](#); [Wosi-](#)
428 [acki and Gobbi, 2012](#)) stated that the direction of littoral drift is preferably
429 to the North, due to the incident waves climate in the region. Regarding the
430 Piçarras, Camboriú and Meia Praia beaches, in Santa Catarina, which showed
431 dominant drift towards the South, this can be explained due to the morphology
432 of the region, which alters the standard alignment of the coast and, consequently,
433 modifies the intensity and direction of action of the waves.

434 For this last stretch, the annual mean sediment transport was lower in Meia
435 Praia (Santa Catarina), reaching $13\,497\text{ m}^3\text{ year}^{-1}$, in addition to Ilha Comprida
436 - São Paulo, with $24\,067\text{ m}^3\text{ year}^{-1}$. On the other hand, in Saquarema and Barra
437 da Tijuca, both in Rio de Janeiro, presented the highest averages occurrence,
438 reaching $690\,670\text{ m}^3\text{ year}^{-1}$ and $625\,670\text{ m}^3\text{ year}^{-1}$, respectively.

439 The variations in the coastal drift observed in all of the analyzed sections
440 from the Brazilian coast can be explained due to the spatial changes in the
441 alignment of the coastline or by the temporal variations of the wave climate
442 itself. [Bittencourt et al. \(2000\)](#) also stated that the presence of coral reefs
443 can act as a barrier, causing in some stretches changes in the drift pattern
444 induced by less intense waves, provoking a reversal in the dominant direction
445 of transport. In order to conclude the evaluation of the longshore sediment
446 transport, the cycles of variability simulated over 37 years was investigated for
447 the entire Brazilian coast, and in order to enforce these results, the wavelet
448 analysis was applied.

449 *3.2. Spatial Variability Analysis*

450 The spatial variability of the longshore sediment transport was analyzed for
451 a transect (which connects the yellow dots in Figure 2), towards the usage of the
452 wavelet analysis. In the two-dimensional analysis, a DOG wavelet (known as
453 Mexican Hat) was considered, following the methodology proposed by Torrence
454 and Compo (1998) and rectified by Liu et al. (2007) and Veeda et al. (2012).

455 At first, all the formulas used in the calculation of sediment transport were
456 investigated, resulting in similar patterns in relation to spatial variability's for
457 cycles between 100 and 1000 days. Thus, for this article, the formulation of
458 CERC (1984), with the parameter K calibrated by Kamphuis et al. (1986),
459 was chosen to compose this analysis, since it represents one of the formulas
460 considered most suitable for the calculation of sedimentary transport in several
461 sectors of the Brazilian coast.

462 Figure 4 (a) shows the local energy spectrum averaged for cycles of vari-
463 ability ranging from 100 to 1000 days, observed over the 37 years simulated
464 and the distance of the Brazilian coast. The average behavior of these cycles is
465 represented by the Hovmöller plot, with the yellow color highlighting the higher
466 energy and frequency of the cycles, while the blue color, shows the situations in
467 which these cycles are less significant and, therefore, do not cause great influence
468 in the longshore sediment transport.

469 The position along the Brazilian coast is indicated on the vertical axis, where
470 the distance of 0 km is related to Arroio Chuí, in the southernmost region of
471 South Brazil, while 6000 km are on Cabo Orange, at the northern end of the
472 Northern Region. The simulation time is shown on the horizontal axis, varying
473 from the year of 1979 to 2015. The mean-integrated variance along space, Figure
474 4 (b), and over time, Figure 4 (c), are also presented.

475 Analyzing the spatial variability along the entire Brazilian coast, Figure 4
476 (a), it can be seen that the cycles of variability between 100 to 1000 days, which
477 are correspondent to annual and interannual cycles of variability, are the most
478 frequent and well defined in some regions, and occur in a transient way in others.

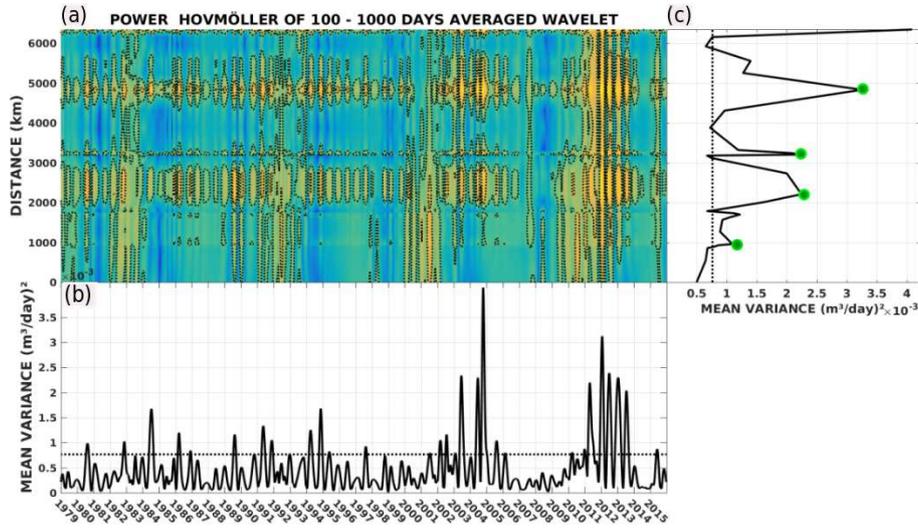


Figure 4: (a) Local energy spectrum for cycles of variability between 100 to 1000 days, observed over time on the Brazilian coast, using the DOG wavelet. Dotted lines indicate the regions with statistical confidence of 95%. (b) Time series of integrated mean variance for all points on the Brazilian coast. The dotted horizontal line represents the level of 95% confidence. (c) Spatial series of mean variance integrated towards the simulation period. The dotted vertical line represents the confidence level 95% while the green points represent the locations where the time variability will be analyzed.

479 At the distances between 2000 and 3000 km, as well as in the stretch of 4500
 480 and 5500 km, these cycles are strongly relevant, indicating a high frequency of
 481 occurrence and higher intensities over the simulated years. These distances are
 482 equivalent to the stretches between the state of Rio de Janeiro and the southern
 483 sector of Bahia, as well as between the western sector of Rio Grande do Norte
 484 and Maranhão.

485 However, in the other stretches, the blue color suggests that the longshore
 486 sediment transport suffers greater influence of the variability cycles shorter than
 487 100 days, being related to the passage of meteorological systems and variations
 488 in the seasonal patterns. For the distance between 0 and 1000 km, correspond-
 489 ing to the section between Rio Grande do Sul and Paraná, 3500 and 4500 km,
 490 between Sergipe and the southeastern sector of Rio Grande do Norte, in addi-
 491 tion to the proximity of 6000 km, in the state of Pará, it can be observed that
 492 the longest cycles are less frequent occurring with greater energy only in some
 493 periods.

494 The spatial integrated mean variance, Figure 4 (b), demonstrates the regions
495 where the occurrence of annual and interannual cycles of variability are most
496 significant across the Brazilian coast, with peaks above the dashed horizontal
497 line having statistical reliability of 95%. The integrated variance over time on
498 the Brazilian coast, Figure 4 (c), confirms the behavior observed in the analysis
499 of the local variability, with peaks at the points where the long period cycles are
500 more intense and frequent, agreeing with the locations shown in Figure 4 (a). It
501 is important to note that, to the right of the dashed vertical line, the reliability
502 of the results are approximately 95%, statistically proving the high influence of
503 annual and interannual cycles at these locations.

504 The annual cycles are associated with changes in the pattern of winds related
505 to the changes of seasons, a fact that is better characterized in some regions the
506 Brazilian coast, as can be observed in the Figures 4 (a) and (b). On the other
507 hand, it stands out the years of 1980, 1982, 1984, 1986, 1989, 1991, 1994, 1997,
508 2002 to 2006, 2010 to 2013 and 2015, when cycles are more intense and energetic.

509 According to data available from National Oceanic and Atmospheric Admin-
510 istration (NOAA⁵), these years are characterized by the occurrence of the El
511 Niño-Southern Oscillation (ENSO) phenomenon, which is defined as the main
512 source of interannual variability in scales of a few years, which represents global
513 impacts as well (Trenberth, 1997; Almeida et al., 2017; Oliveira et al., 2017).

514 A greater disparity is observed, in the year of 2004, in comparison to the
515 other periods, being able to be related to the passage of a tropical cyclone
516 coming from the South Atlantic, known as "Hurricane Catarina" (Dias et al.,
517 2004; Menezes and Dias, 2004), that reached the coast of South Region of Brazil
518 in March, producing winds above 30 m s^{-1} (Menezes and Dias, 2004). Another
519 extreme event, known as the "Ribeirão Preto Case", occurred in May 1994, when
520 severe convective storms formed over the state of São Paulo, causing strong
521 winds and hail, with gusts reaching velocities higher than 28 m s^{-1} (Menezes

⁵http://origin.cpc.ncep.noaa.gov/products/analysis_monitoring/ensostuff/ONI_v5.php

522 and Dias, 1998, 2004).

523 In this way, it is important to emphasize that cyclones are the atmospheric
524 systems that produce the most extreme winds where they are, being their in-
525 fluence in the South Atlantic Ocean quite common (Dereczynski and Menezes,
526 2015), in addition they are able to cause, directly and indirectly, significantly
527 variations in the sediment transport. Additionally, the severity of events can be
528 intensified over the years influenced by interannual events.

529 Another factor related to the integrated energy towards time, refers to the
530 intensification and propagation of the cycles of 100 to 1000 days after the 90th
531 decade, standing out the period from 2010, that is clearly the most energetic.
532 Such occurrence might be addressed in a future study proposal, in which the
533 causes of the intensification of the long period cycles in the last years shall be
534 enlighten.

535 3.3. Temporal Variability Analysis

536 The wavelet method also allowed the analysis of the temporal variability
537 of longshore sediment transport along the Brazilian coast. For this analysis,
538 four points were selected located in Galinhos - Rio Grande do Norte, Salvador
539 - Bahia, Praia do Açú - Rio de Janeiro and Balneário Barra do Sul - Santa
540 Catarina, which are indicated by the circles of green color in Figures 2 and 4
541 (c).

542 The longshore sediment transport formula considered more adequate for each
543 site was used with the one-dimensional DOG wavelet, following the methodology
544 proposed by Torrence and Compo (1998) and rectified by Liu et al. (2007) and
545 Veeda et al. (2012). Figures 5 and 6 demonstrated the time series of sediment
546 transport (in $\text{m}^3 \text{d}^{-1}$) during the simulated 37 years.

547 The predominance of positive values indicates that the coastal drift is dom-
548 inant to the West or North, depending on the position of the point, while the
549 negative values represent the drift towards East or South. In addition, the local
550 spectrum measures the amount of energy over the time for the cycles of vari-

551 ability occurring between 8 and 4096 days, the most energetic situations being
 552 those in which the red color and the black outline become more evident. The
 553 global spectrum complements the results visualized, indicating the cycles that
 554 most influence the longshore sediment transport in an integrated way.

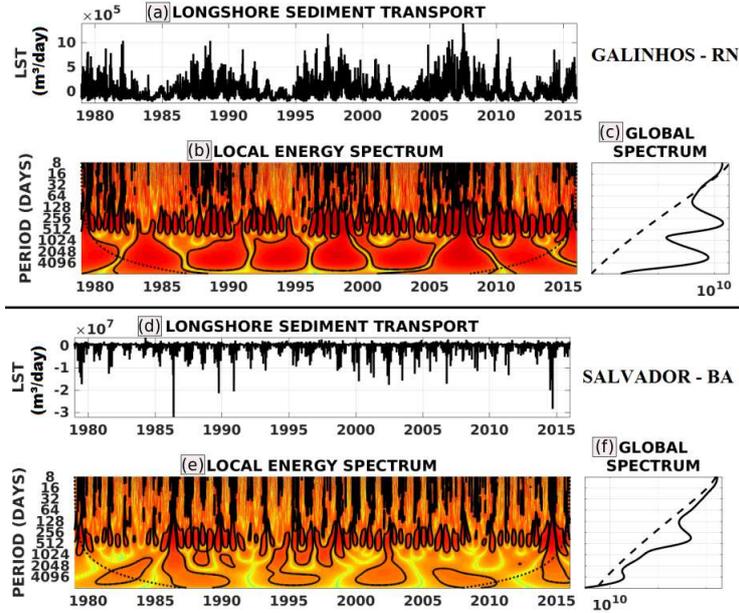


Figure 5: (a) and (d) Analysis of the Wavelet Method represented by the time series of longshore sediment transport in Galinhos - Rio Grande do Norte and Salvador - Bahia. (b) and (e) The local energy spectrum, and the black outlines represent the confidence level of 95% and the black dotted line represents the cone of influence. (c) and (f) The overall energy spectrum, and the black dotted line indicates the level of 95% confidence.

555 Figure 5 (a) presents the time series at Galinhos - Rio Grande do Norte,
 556 and it is observed peaks in sediment transport throughout the period, being
 557 the largest between years 2005 and 2010. It may also be noted that there is a
 558 variation between peaks, which increase and decrease approximately at every 5
 559 years. In addition, the predominance of positive values in the series confirms
 560 the western direction of the coastal drift, as discussed above.

561 The local energy spectrum is represented by the red color and the black
 562 outline, presented in Figure 5 (b), and it shows that the highest energy concen-
 563 trations occurred between 256 and 2048 days. These cycles can be associated
 564 with annual and interannual cycles, which are characterized by ENSO. This

565 dominance of the longest cycles in longshore sediment transport has also been
566 demonstrated for this point.

567 In addition, it can be observed that the seasonal and intra-annual cycles, be-
568 tween 128 and 256 days, also influence the transport, representing the variations
569 caused by the passages of the seasons. The black color also highlights the high
570 energy related to the short period cycles, between 8 and 128 days, however, in
571 the global context of the long period analysis, these cycles are the less energetic.

572 The high energy rate associated with the medium and long-term phenomena
573 is in agreement with the result presented in the global spectrum, in the Figure 5
574 (c). This result also shows that the shorter cycles do not exert a great influence
575 on the longshore sediment transport when compared to the longer cycles.

576 The time series of longshore sediment transport in Salvador - Bahia are
577 presented in the Figure 5 (d). This result demonstrates that isolated peaks
578 have occurred in transport over the years, with the largest of them between 1985
579 and 1990 and around 2015. In the other years, the series remained practically
580 constant, with coastal drift permanently dominant towards South, as expected,
581 due to the predominance of negative values.

582 The local spectrum is presented in the Figure 5 (e), and it is observed that
583 highest energy concentrations for the cycles occurred between 128 and 512 days,
584 over the 37 years simulated. This result demonstrates that seasonal and annual
585 cycles effects are the ones that most influence the longshore sediment transport
586 towards this region. In this way, this fact is corroborated by the global energy
587 spectrum, presented in the Figure 5 (f).

588 In addition, the interannual cycles are well defined in some periods such
589 as the years 1989, 1995, 2003 and 2007, which according to NOAA are years
590 influenced by ENSO. In relation to the short period cycles, these were energetic
591 and frequent throughout all years, losing their relevance due to the amount of
592 energy associated with the longer cycles.

593 For the point in Praia do Açú - Rio de Janeiro, it is observed a high dis-
594 crepancy of peaks along the time series, according to Figure 6 (a). The 90's is

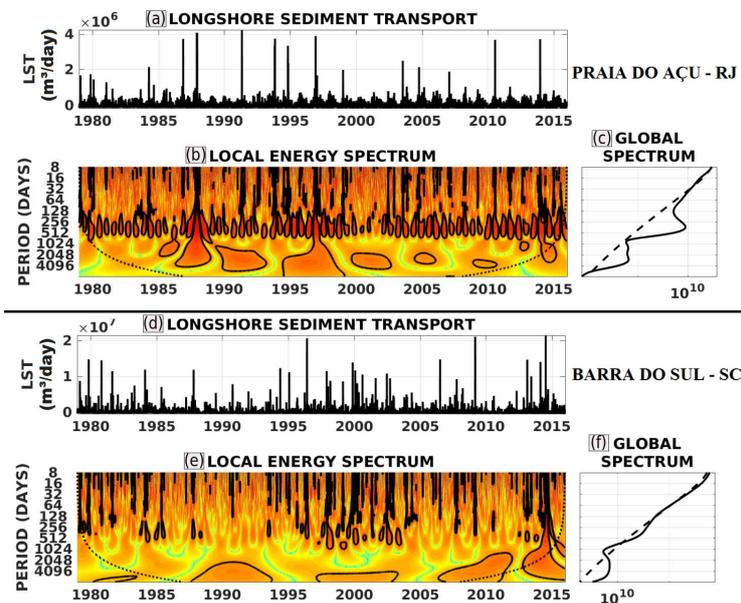


Figure 6: (a) and (d) Analysis of the Wavelet Method represented by the time series of longshore sediment transport in Praia do Açu - Rio de Janeiro and Balneário Barra do Sul - Santa Catarina. (b) and (e) The local energy spectrum, and the black outlines represent the confidence level of 95% and the black dotted line represents the cone of influence. (c) and (f) The overall energy spectrum, and the black dotted line indicates the level of 95% confidence.

595 highlighted because the peaks were higher and with a higher frequency. Coastal
 596 drift was dominant for the North, since positive values prevailed in the series.

597 The local spectrum is presented in the Figure 6 (b) and it shows that the
 598 most energetic cycles refers to the period between 128 and 512 days, with pre-
 599 dominance over the 37 years analyzed. The cycles greater than 512 days are
 600 also energetic and influence the longshore sediment transport.

601 Starting from 1985, highlighting the period between 1995 and 2000, it is
 602 possible to observe the occurrence of a well-defined interannual phenomenon,
 603 according to the time series. The shorter cycles show few relevance for this
 604 point, although they also occur over the years.

605 Finally, the global spectrum presented in the Figure 6 (c) highlights that
 606 annual and interannual cycles are the most important in longshore sediment
 607 transport and that shorter cycles are not significant at this time scale. It is
 608 important to emphasize that local and global energy spectra showed a similar
 609 behavior that occurred in Salvador, as shown previously in Figure 4.

610 For the last point, located in the Balneário Barra do Sul - Santa Catarina,
611 the time series demonstrated a high variability of the peaks along the 37 years,
612 not following any pattern. This result can be observed in the Figure 6 (d).

613 Nearby the years of 1996, 2009 and 2015, the highest values occurred, being
614 these associated to the occurrence of El Niño and La Niña events, according to
615 NOAA. In addition, the predominance of positive values in the series represents
616 that the coastal drift is towards the North.

617 The local and global energy spectra are presented in the Figures 6 (e) and
618 (f), and its show an extremely different behavior in relation to the other points
619 analyzed. In the local spectrum is observed that cycles greater than 128 days do
620 not present an amount of energy so different when compared to smaller cycles
621 between 8 and 32 days.

622 The intensity of shorter cycles is greater because in the southernmost re-
623 gions of Brazil the passage of meteorological systems occurs more frequently
624 and intensely than in other regions, significantly affecting sediment transport
625 and interfering with the pattern of variability on a seasonal and annual scale. It
626 can also be observed that the interannual cycles are more energetic in the years
627 1990, 2000 and 2010, reflecting their relevance in the global spectrum, according
628 to Figure 6 (f).

629 Thus, the shorter cycles always occur and are energetic as the others, how-
630 ever, it is possible to conclude that for the global context of the analysis, the
631 annual and interannual cycles are the most important for the control of long-
632 shore sediment transport. In addition, it can be emphasized that the interan-
633 nual cycles contribute to a more frequently and well defined longshore sediment
634 transport in the northeast and north of the Brazilian coast.

635 4. Conclusions

636 Considering the numerical modeling of the waves generated by the wind
637 during a period of 37 years, it was possible to estimate the annual means of
638 sediment transport for 85 points along the entire Brazilian coast. The four

639 methodologies applied in the calculations proved to be satisfactory, with the
640 exception of the formulation of CERC (1984), with the parameter K equals
641 to 0.39, which was not suitable for any region. The formulation of Kamphuis
642 (1991) was applied in most of the points, however, the formulation of CERC
643 (1984), with the K calibrated by Kamphuis et al. (1986), covered most of the
644 Brazilian coast.

645 In relation to the obtained sedimentary rates, the highest occurred in the
646 Northeast Region of Brazil, emphasizing the sector between Pina (Pernambuco)
647 and Piaçabuçu (Alagoas), with averages up to $844\,320\text{ m}^3\text{ year}^{-1}$. Another sec-
648 tor that presented high transport values refers to Maraú and Ilhéus, both in
649 Bahia, with an average of approximately $650\,000\text{ m}^3\text{ year}^{-1}$.

650 In the state of Rio de Janeiro, Saquarema and Barra da Tijuca stood out,
651 with values closer to $690\,000\text{ m}^3\text{ year}^{-1}$. On the other hand, the lowest averages
652 occurred in different analyzed regions, the lowest in Meia Praia (Santa Catarina)
653 with $13\,497\text{ m}^3\text{ year}^{-1}$, followed by Mucuri (Bahia) with $22\,577\text{ m}^3\text{ year}^{-1}$, and
654 Ilha Comprida (São Paulo) with $24\,067\text{ m}^3\text{ year}^{-1}$.

655 Although only three sedimentary fractions were considered to characterize
656 the sedimentology of the study region, these were appropriate for each stretch,
657 since they did not affect the results very significantly. In fact, it is suggested
658 that in future studies a more refined sedimentological data set should be used,
659 further improving the results. In addition, the choice of other formulas to cal-
660 culate sediment transport can also be considered, allowing a comparison with
661 the results presented in this article.

662 The spatial and temporal variability analysis presented important aspects in
663 relation to the influence of variability cycles in the longshore sediment transport.
664 For the northern regions of Brazil, the interannual cycles were more frequent
665 and energetic than in the southern regions of Brazil, where shorter cycles were
666 significant also.

667 The high frequency of the annual and interannual cycles during the 37 years
668 occurred in the sector between Maranhão and Rio Grande do Norte, as well

669 as between Bahia and Rio de Janeiro. In the other stretches of the Brazilian
670 region, these cycles of long period occurred transiently, being masked by cycles
671 of shorter period.

672 In addition, the high intensity and energy of the long period cycles were
673 also observed in the years of 1980, 1982, 1984, 1986, 1989, 1991, 1994, 1997,
674 2002 to 2006, 2010 to 2013 and 2015, being related to the occurrence of the
675 ENSO phenomenon. After the 90th, the intensification and the increase in the
676 frequency of these cycles can also be verified, highlighting the year of 2010,
677 when it becomes evident that these events have become more energetic. This
678 fact also makes possible a future study to clarify the causes of the intensification
679 and increase in the frequency of occurrence of the interannual cycles in recent
680 years.

681 The temporal variability analysis of the transport also allowed the conclusion
682 that the short period cycles, related to the passage of meteorological systems,
683 are always present throughout the year in the different regions, especially the
684 south region that is strongly affected by the action of low pressure atmospheric
685 features. However, such cycles lose their relevance as mechanisms to promote
686 sediment transport when compared to annual and interannual cycles, which
687 carry a greater amount of energy and, therefore, become more significant in the
688 scale of variability of this study.

689 Thus, the present article contributes with relevant information about long-
690 shore sediment transport, highlighting the annual averages and the dominant
691 drift, along the entire Brazilian coast. In addition, important questions about
692 the influence of cycles of variability in the study region are discussed, empha-
693 sizing the importance of the longer period events for the control of sedimentary
694 transport in the Brazilian coast.

695 **5. Acknowledgments**

696 The authors would like to thanks the ECMWF by oceanographic and me-
697 teorological data used in the model boundary conditions, the consortium Open

698 TELEMAC-MASCARET by providing the TELEMAC system charge, the Na-
699 tional Laboratory of Scientific Computing (LNCC) by making use of the super-
700 computer Santos Dumont and Centro Nacional de Supercomputação (CESUP)
701 of Federal University of Rio Grande do Sul (UFRGS) for supporting the devel-
702 opment of this research. This study was financed in part by the *Coordenação de*
703 *Aperfeiçoamento de Pessoal de Nível Superior* (CAPES), Brazil - Finance Code
704 001, and was supported by the *Fundação de Amparo à Pesquisa do Estado do*
705 *Rio Grande do Sul* (FAPERGS), Brazil - Contract 17/2551-001159-7, and by
706 the *Conselho Nacional de Desenvolvimento Científico e Tecnológico* (CNPq),
707 Brazil - Contract 304227/2016-1.

708 A. H. d. F. Klein, J. T. Menezes, F. L. Diehl, J. G. N. de Abreu, M. Polette,
709 R. M. Sperb, R. C. Sperb, N. Horn, Santa Catarina, in: D. Muehe (Ed.),
710 *Erosão e Progradação do Litoral Brasileiro Litoral Brasileiro*, Ministério do
711 Meio Ambiente (MMA), Brasília, 2006, pp. 401–436.

712 CERC, *Shore Protection Manual*, 4 ed., U.S. Army Coastal Engineering Re-
713 search Center, Washington, D. C., 1984.

714 L. H. Holthuijsen, *Waves in Oceanic and Coastal Waters*, 1 ed., Cambridge
715 University Press, Cambridge, 2007.

716 I. R. Silva, A. C. d. S. P. Bittencourt, J. M. L. Dominguez, *Modelagem de*
717 *Ondas como Subsídio para a Gestão Ambiental das Praias da Costa do De-*
718 *scobrimento, Sul do Estado da Bahia*, Simpósio Brasileiro de Sensoriamento
719 Remoto (2007) 4691–4697.

720 L. Giosan, H. Bokuniewicz, N. Panin, I. Postolache, *Longshore Sediment Trans-*
721 *port Pattern along Romanian Danube Delta Coast*, Marine Geosciences Cen-
722 ter (1996).

723 V. S. Kumar, P. Pednekar, P. Chandramohan, K. a. Kumar, R. Gowthaman,
724 *Longshore Currents and Sediment Transport along Kannirajapuram Coast,*
725 *Tamilnadu, India*, *Journal of Coastal Research* 16 (2000) 247–254.

- 726 F. S. B. F. Oliveira, T. C. A. Oliveira, R. Silva, S. H. C. D. Larangeiro, Dinâmica
727 sedimentar do trecho litoral praia da vieira - praia velha - hidrodinâmica e
728 transporte longitudinal de sedimentos, in: VII Congresso da Água, 2004,
729 p. 15.
- 730 A. C. D. S. P. Bittencourt, J. M. L. Dominguez, L. Martin, I. R. Silva, Longshore
731 transport on the northeastern Brazilian coast and implications to the location
732 of large scale accumulative and erosive zones: An overview, *Marine Geology*
733 219 (2005) 219–234. doi:[10.1016/j.margeo.2005.06.006](https://doi.org/10.1016/j.margeo.2005.06.006).
- 734 M. R. Moura, J. O. Morais, Análise do balanço sedimentar da faixa de praia do
735 litoral oeste de aquiraz, ceará, *Revista de Geologia* 24 (2011) 187–198.
- 736 T. C. A. Oliveira, J. Albino, I. Venancio, Transporte longitudinal
737 de sedimentos no litoral da planície deltaica do Rio Doce, *Qua-*
738 *ternary and Environmental Geosciences* 6 (2015) 20 – 25. URL:
739 <http://revistas.ufpr.br/abequa/article/view/36738/25076>.
740 doi:<http://dx.doi.org/10.5380/abequa.v6i1.36738>.
- 741 G. V. Silva, E. E. Toldo, A. H. d. F. Klein, A. D. Short, C. D. Woodroffe, Head-
742 land Sand Bypassing - Quantification of Net Sediment Transport in Embayed
743 Beaches, Santa Catarina Island North Shore, Southern Brazil, *Marine Geol-*
744 *ogy* 379 (2016) 13–27. URL: [http://dx.doi.org/10.1016/j.margeo.2016.](http://dx.doi.org/10.1016/j.margeo.2016.05.008)
745 [05.008](http://dx.doi.org/10.1016/j.margeo.2016.05.008). doi:[10.1016/j.margeo.2016.05.008](https://doi.org/10.1016/j.margeo.2016.05.008).
- 746 T. B. Trombetta, R. C. Guimarães, J. Costi, W. C. Marques, An overview
747 of longshore sediment transport on the brazilian coast, *Regional Studies in*
748 *Marine Science* 35 (2020).
- 749 A. D. Short, A. H. d. F. Klein, *Brazilian Beach Systems*, Springer Nature, Boca
750 Raton , Flórida, EUA, 2016.
- 751 M. G. Tessler, S. C. Goya, Processos Costeiros Condicionantes do Litoral
752 Brasileiro, *Revista do Departamento de Geografia* 17 (2005) 11–23.

753 URL: <http://www.revistas.usp.br/rdg/article/view/47271>. doi:10.
754 [7154/RDG.2005.0017.0001](https://doi.org/10.1154/RDG.2005.0017.0001).

755 M. Benoit, F. Marcos, F. Becq, Development of a Third Generation Shallow-
756 Water Wave Model with Unstructured Spatial Meshing, in: 25th International
757 Conference on Coastal Engineering: Book of Abstracts, American Society of
758 Civil Engineers, New York, 1996, pp. 465–478.

759 S. Hasselmann, K. Hasselmann, E. Bauer, P. A. E. M. Janssen,
760 G. J. Komen, L. Bertotti, P. Lionello, A. Guillaume, V. C. Car-
761 done, J. A. Greenwood, M. Reistad, L. Zambresky, J. A. Ew-
762 ing, The WAM Model - A Third Generation Ocean Wave Pre-
763 diction Model, Journal of Physical Oceanography 18 (1988) 1775–
764 1810. URL: [http://journals.ametsoc.org/doi/abs/10.1175/
765 1520-0485\(1988\)018<1775:TWMTGO>2.0.CO;2](http://journals.ametsoc.org/doi/abs/10.1175/1520-0485(1988)018<1775:TWMTGO>2.0.CO;2).
766 doi:10.1175/1520-0485(1988)018<1775:TWMTGO>2.0.CO;2.

767 L. H. Holthuijsen, N. Booji, I. J. G. Haagsma, Comparing 1st, 2nd and 3rd
768 Generation Wave Modelling, in: Proceedings of 26th Conference on Coastal
769 Engineering, American Society of Civil Engineers, Copenhagen, 1998, pp.
770 140–149. doi:10.1061/9780784404119.

771 T. Awk, Tomawac User Manual Version 7.2, 2017. URL: www.opentelemac.org.

772 J. W. Kamphuis, Alongshore Sediment Transport Rate, Journal of Waterway,
773 Port, Coastal, and Ocean Engineering 117 (1991) 624.

774 S. F. Lima, L. E. Almeida, E. E. Toldo Júnior, Estimativa da Capacidade de
775 Transporte Longitudinal de Sedimentos a partir de Dados de Ondas para a
776 Costa do Rio Grande do Sul, Pesquisas em Geociências 28 (2002) 99–107.

777 J. W. Kamphuis, M. H. Davies, R. B. Nairn, O. J. Sayao, Calculation of lit-
778 toral sand transport rate, Coastal Engineering 10 (1986) 1–21. doi:10.1016/
779 0378-3839(86)90036-0.

- 780 J. Mil-Homens, R. Ranasinghe, J. S. M. van Thiel de Vries, M. J. F. Stive,
781 Re-evaluation and Improvement of Three Commonly Used Bulk Longshore
782 Sediment Transport Formulas, *Coastal Engineering* 75 (2013) 29–39.
- 783 C. Torrence, G. P. Compo, *A Practical Guide to Wavelet Analysis*, American
784 Meteorological Society 79 (1998) 61–78.
- 785 Y. Liu, X. S. Liang, R. H. Weisberg, Rectification of the Bias in the Wavelet
786 Power Spectrum, *Journal of Atmospheric and Oceanic Technology* 24 (2007)
787 2093–2102.
- 788 D. Veleda, R. Montage, M. Araujo, Cross-Wavelet Bias Corrected by Nor-
789 malizing Scales, *Journal of Atmospheric and Oceanic Technology* 29 (2012)
790 1401–1408.
- 791 E. d. P. Kirinus, P. H. Oleinik, J. Costi, W. C. Marques, Long-term
792 simulations for ocean energy off the Brazilian coast, *Energy* 163 (2018)
793 364 – 382. URL: [http://www.sciencedirect.com/science/article/
794 pii/S0360544218316128](http://www.sciencedirect.com/science/article/pii/S0360544218316128). doi:[https://doi.org/10.1016/j.energy.2018.
795 08.080](https://doi.org/10.1016/j.energy.2018.08.080).
- 796 R. C. Guimarães, P. H. Oleinik, E. d. P. Kirinus, B. V. Lopes, T. B. Trom-
797 betta, W. C. Marques, An overview of the Brazilian continental shelf
798 wave energy potential, *Regional Studies in Marine Science* 25 (2019)
799 100446. URL: [http://www.sciencedirect.com/science/article/pii/
800 S235248551830152X](http://www.sciencedirect.com/science/article/pii/S235248551830152X)[http://www.swge.inf.br/proceedings/paper/?P=
801 CILAMCE2017-0701](http://www.swge.inf.br/proceedings/paper/?P=CILAMCE2017-0701). doi:[10.20906/CPS/CILAMCE2017-0701](https://doi.org/10.20906/CPS/CILAMCE2017-0701).
- 802 A. M. T. Marcelino, L. R. d. S. G. Pinheiro, J. R. S. Costa, Planejamento partic-
803 ipativo para a gestão da orla marítima de Galinhos/RN, nordeste brasileiro,
804 com apoio de sensores remotos e modelagem costeira, *Revista Desenvolvi-
805 mento e Meio Ambiente* 44 (2018) 118–139.
- 806 D. J. C. Araújo, *Transporte Longitudinal De Sedimento Na Zona Costeira De*
807 *Natal RN, Dissertação, Universidade Federal do Rio Grande do Norte, 2015.*

- 808 N. Contti Netto, Deriva litorânea e evolução da linha de costa no sul do Espírito
809 Santo (Brasil), Thesis, Instituto Oceanográfico, Universidade de São Paulo,
810 2013.
- 811 A. C. Bastos, C. G. Silva, Caracterização morfodinâmica do litoral Norte Flumi-
812 nense, RJ, Brasil, Revista Brasileira de Oceanografia 48 (2000) 41–60. doi:[10.
813 1002/1097-4679\(195004\)6:2<203::AID-JCLP2270060224>3.0.CO;2-Q](https://doi.org/10.1002/1097-4679(195004)6:2<203::AID-JCLP2270060224>3.0.CO;2-Q).
- 814 R. Araújo, P. Alfredini, O Cálculo do Transporte de Sedimentos Litorâneo:
815 Estudo de Caso das Praias de Suarão e Cibratel (Município de Itanhaém ,
816 São Paulo), RBRH - Revista Brasileira de Recursos Hídricos 6 (2001) 15–28.
- 817 L. F. K. Wosiacki, M. F. Gobbi, Estimativa do Transporte de Sedimentos
818 na Praia Brava de Matinhos/PR com auxílio da Modelagem Numérica das
819 Ondas, in: V Seminário e Workshop em Engenharia Oceânica, Universidade
820 Federal do Rio Grande, Rio Grande, 2012.
- 821 J. A. Castilhos, J. C. R. Gré, Beach Morphodynamics and Sediment Trans-
822 port along the Northern Coast of Santa Catarina, Brazil, Journal of Coastal
823 Research SI 1 (2006) 1756–1761.
- 824 L. J. Calliari, A. H. Klein, Características Morfodinâmicas e Sedimentológicas
825 das Praias Oceânicas Entre Rio Grande e Chuí, RS, Pesquisas em Geociências
826 20 (1993) 45–56.
- 827 R. C. Barletta, Efeito da interação oceano- atmosfera sobre a morfodinâmica
828 das praias do litoral, Ph.D. thesis, Universidade Federal do Rio Grande, 2000.
- 829 E. Siegle, N. E. Asp, Wave Refraction and Longshore Transport
830 Patterns Along the Southern Santa Catarina Coast, BRAZILIAN
831 JOURNAL OF OCEANOGRAPHY 55 (2007) 109–120. doi:[10.1590/
832 S1679-87592007000200004](https://doi.org/10.1590/S1679-87592007000200004).
- 833 C. T. Martinho, S. R. Dillenburg, P. Hesp, Wave Energy and Longshore Sed-
834 iment Transport Gradients Controlling Barrier Evolution in Rio Grande do

- 835 Sul, Brazil, *Journal of Coastal Research* 252 (2009) 285–293. URL: <http://www.bioone.org/doi/abs/10.2112/06-0645.1>. doi:10.2112/06-0645.1.
- 836
- 837 G. R. McGregor, S. Nieuwolt, *Tropical Climatology: An Introduction to the*
- 838 *Climates of the Low Latitudes*, 1 ed., Wiley, New York, 1998.
- 839 J. M. L. Dominguez, The Coastal Zone of Brazil: an overview, in: S. R. Dillen-
840 lenburg, P. A. Hesp (Eds.), *Geology and Geomorphology of Holocene Coastal*
841 *Barriers of Brazil*, Springer, Berlin, 2009, pp. 16 – 20.
- 842 F. S. B. F. Oliveira, Wave climate modelling south of rio de janeiro in
843 brazil, *Continental Shelf Research* 22 (2002) 2021 – 2034. URL: <http://www.sciencedirect.com/science/article/pii/S0278434302000456>.
844 doi:[https://doi.org/10.1016/S0278-4343\(02\)00045-6](https://doi.org/10.1016/S0278-4343(02)00045-6).
- 845
- 846 C. Pianca, P. L. F. Mazzini, E. Siegle, Brazilian Offshore Wave Climate based
847 on NWW3 Reanalysis, *Brazilian Journal of Oceanography* 58 (2010) 53–70.
- 848 R. L. Espindola, A. M. Araújo, Wave Energy Resource of Brazil: An Analysis
849 from 35 years of ERA-Interim Reanalysis Data, *PLOS ONE* (2017).
- 850 D. Muehe, Estado morfodinâmico praias no instante da observação:
851 uma alternativa de identificação, *Revista Brasileira de Oceanografia*
852 46 (1998) 157–169. URL: [http://www.scielo.br/scielo.php?script=](http://www.scielo.br/scielo.php?script=sci_arttext&pid=S1413-77391998000200005&nrm=iso)
853 [sci_{_}arttext{&}pid=S1413-77391998000200005{&}nrm=iso](http://www.scielo.br/scielo.php?script=sci_arttext&pid=S1413-77391998000200005&nrm=iso).
- 854 D. d. F. Gurgel, *Modelagem do Transporte de Sedimentos na Zona Costeira da*
855 *Barreira do Inferno-RN, Através do SMC-Brasil*, Ph.D. thesis, Universidade
856 Federal do Rio Grande Do Norte, 2017.
- 857 A. C. S. P. Bittencourt, L. Martin, J. M. L. Dominguez, I. R. Silva, D. L.
858 Sousa, A significant longshore transport divergence zone at the North-
859 eastern Brazilian coast: Implications on coastal Quaternary evolution,
860 *Anais da Academia Brasileira de Ciências* 74 (2002) 505–518. doi:10.1590/
861 [S0001-37652002000300012](https://doi.org/10.1590/S0001-37652002000300012).

- 862 A. C. Bittencourt, Z. M. Leão, R. K. Kikuchi, J. M. Domínguez, Deficit of
863 sand in a sediment transport model favors coral reef development in Brazil,
864 Anais da Academia Brasileira de Ciências 80 (2008) 205–214. doi:[10.1590/
865 S0001-37652008000100015](https://doi.org/10.1590/S0001-37652008000100015).
- 866 A. C. D. S. P. Bittencourt, J. M. L. Dominguez, L. Martin, I. R. Silva,
867 Patterns of sediment dispersion coastwise the State of Bahia - Brazil,
868 Anais da Academia Brasileira de Ciências 72 (2000) 271–287. doi:[10.1590/
869 S0001-37652000000200012](https://doi.org/10.1590/S0001-37652000000200012).
- 870 J. C. M. Cassar, C. F. Neves, Aplicação das rosas de transporte litorâneo à
871 costa fluminense, Revista Brasileira de Engenharia 11 (1993) 81–106.
- 872 K. M. Machado, A. R. Alves, G. B. Fernandez, Clima de Ondas e Transporte
873 Litorâneo na Planície Deltaica do Rio Paraíba do Sul, Litoral Norte do estado
874 do Rio de Janeiro, in: III Encontro Latino Americano de Geomorfologia, 2018,
875 pp. 1–15.
- 876 E. F. Gobbi, Gerenciamento Costeiro: Análise de casos do litoral do Paraná sob
877 a perspectiva da Engenharia Costeira, Ph.D. thesis, Universidade Federal do
878 Rio de Janeiro, 1997.
- 879 F. A. Veiga, R. J. Angulo, E. Marone, F. P. Brandini, Características sedimen-
880 tológicas da plataforma continental interna rasa na porção central do Litoral
881 Paranaense, Boletim Paranaense de Geociências 55 (2004) 67–75.
- 882 C. A. Thoaldo, Transporte de sedimentos na costa do Paraná, Ph.D. thesis,
883 Universidade Federal do Paraná, 2011.
- 884 J. J. Abreu, Transporte Sedimentar Longitudinale Morfodinâmica Praial: Ex-
885 emplo do Litoral Norte de Santa Catarina, Ph.D. thesis, Universidade Federal
886 de Santa Catarina, 2011.
- 887 K. Trenberth, The definition of el niño, Bulletin of the American Meteorological
888 Society 78 (1997) 2771–2777.

- 889 C. T. Almeida, J. F. Oliveira-Júnior, R. C. Delgado, P. Cubo, M. C.
890 Ramos, Spatiotemporal rainfall and temperature trends through-
891 out the brazilian legal amazon 1973–2013, International Jour-
892 nal of Climatology 37 (2017) 2013–2026. doi:10.1002/joc.4831.
893 arXiv:<https://rmets.onlinelibrary.wiley.com/doi/pdf/10.1002/joc.4831>.
- 894 M. J. d. Oliveira, C. D. R. Carneiro, F. A. d. S. Vecchia, G. M. d. M. Baptista,
895 Ciclos climáticos e causas naturais das mudanças do clima, Terrae Didactica 13
896 (2017) 149–184. URL: <https://periodicos.sbu.unicamp.br/ojs/index.php/td/article/view/8650958>. doi:10.20396/td.v13i3.8650958.
- 898 P. S. Dias, M. Dias, M. Seluchi, F. Diniz, O ciclone catarina: análise preliminar
899 da estrutura, dinâmica e previsibilidade, in: Anais do XI Congresso Brasileiro
900 de Meteorologia, 2004.
- 901 W. F. Menezes, M. A. F. d. S. Dias, Aspectos termodinâmicos de sistemas de
902 baixas pressões profundas associadas a tempestades: uma comparação entre
903 os casos “Ribeirão Preto” e “Catarina”, in: Anais do XI Congresso Brasileiro
904 de Meteorologia, 2004.
- 905 W. F. Menezes, M. A. F. d. S. Dias, Simulação numérica das tempestades
906 ocorridas no estado de São Paulo em 14 de maio de 1994: O caso Ribeirão
907 Preto, in: Anais do X Congresso Brasileiro de Meteorologia, 1998.
- 908 C. P. Dereczynski, W. F. Menezes, Meteorologia da Bacia de Campos, in: R. P.
909 Martins, G. S. Grossman-Matheson (Eds.), Caracterização ambiental regional
910 da Bacia de Campos, Atlântico Sudoeste: Meteorologia e Oceanografia. Habi-
911 tats, v.2 ed., Elsevier Ltd, Rio de Janeiro, Brazil, 2015, pp. 1–54.

Figures

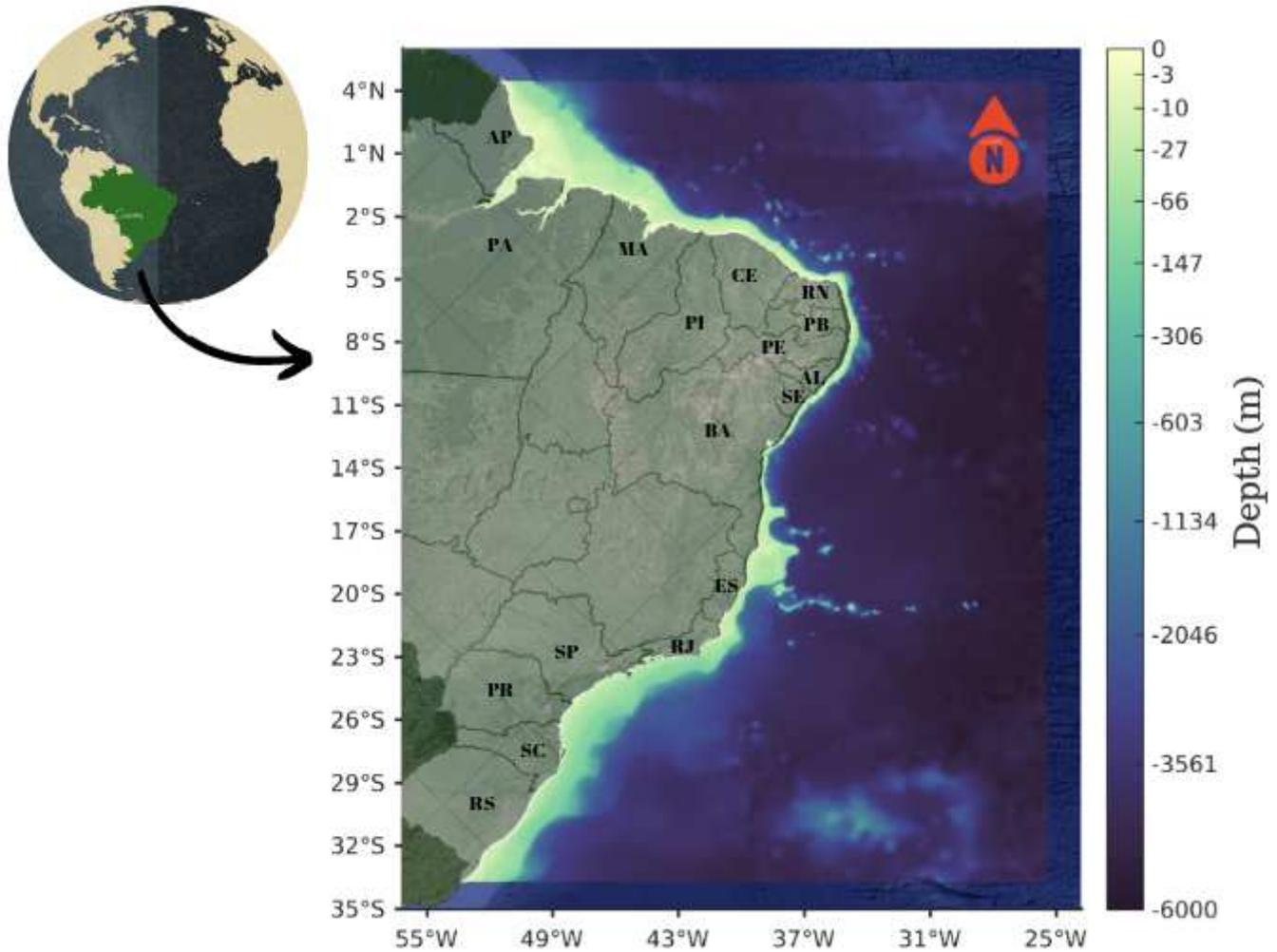


Figure 1

Representation of the study area, with bathymetric data and pointing coastal states - Amapá (AP), Pará (PA), Maranhão (MA), Piauí (PI), Ceará (CE), Rio Grande do Norte (RN), Paraíba (PB), Pernambuco (PE), Alagoas (AL), Sergipe (SE), Bahia (BA), Espírito Santo (ES), Rio de Janeiro (RJ), São Paulo (SP), Paraná (PR), Santa Catarina (SC) and Rio Grande do Sul (RS). The colorbar represents the depth in meters.

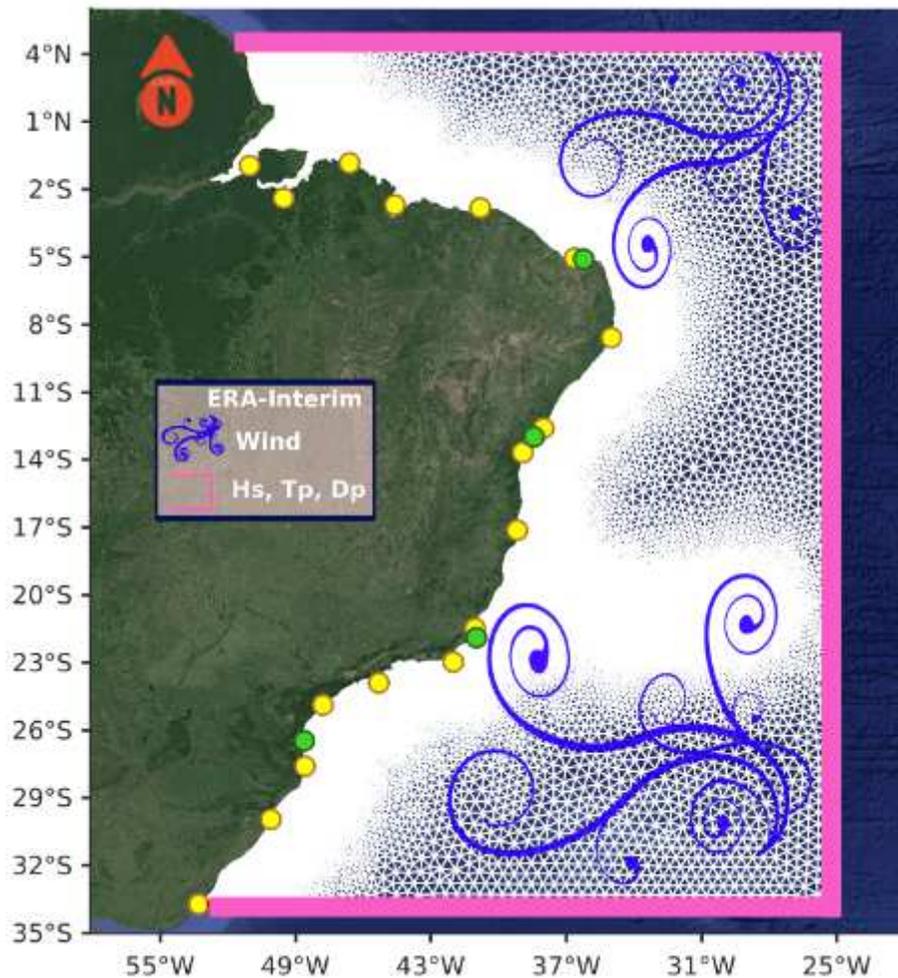


Figure 2

Figure of the computational domain with surface and boundary conditions. The points represent the areas used to analyze the spatial (in yellow) and temporal (in green) variability. The pink lines and the blue symbols represent wave and wind data, respectively.

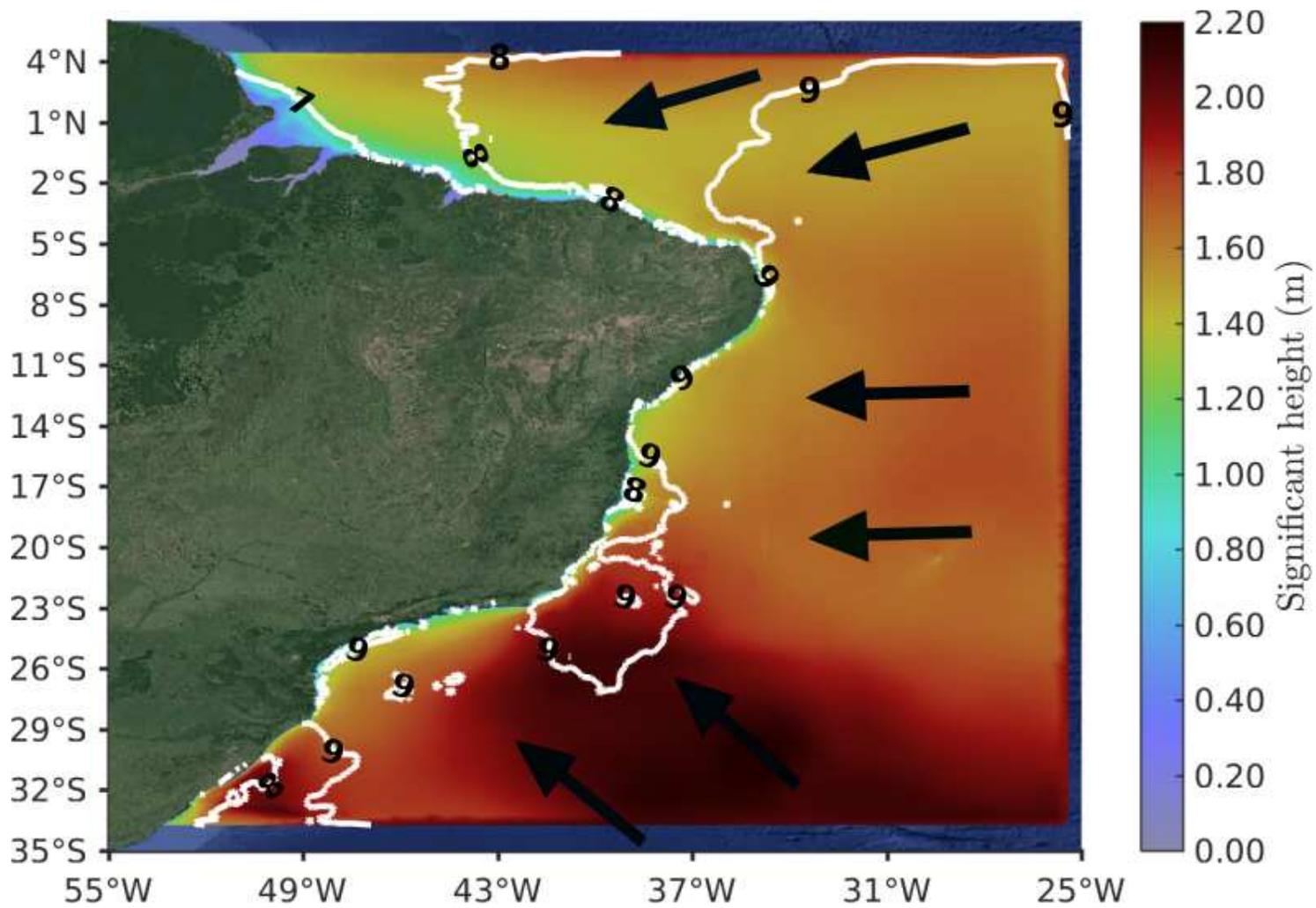


Figure 3

Results of the Brazilian Continental Shelf, overlapping image by Google Maps, Landsat/Copernicus, 2018. Frame shows H_s (m) in the surface, T_p (s) in the isolines and M_d in the arrows.

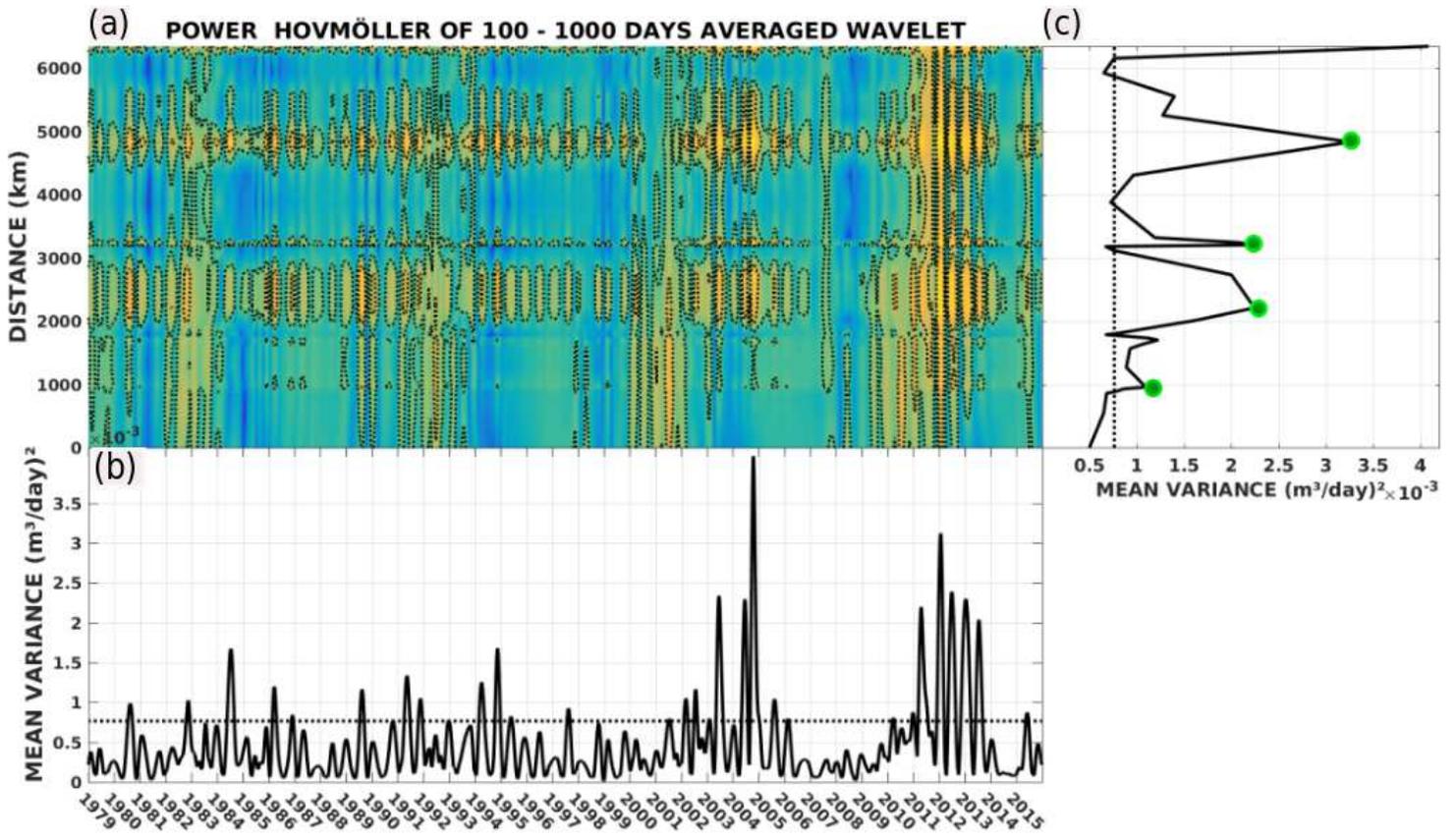


Figure 4

(a) Local energy spectrum for cycles of variability between 100 to 1000 days, observed over time on the Brazilian coast, using the DOG wavelet. Dotted lines indicate the regions with statistical confidence of 95%. (b) Time series of integrated mean variance for all points on the Brazilian coast. The dotted horizontal line represents the level of 95% confidence. (c) Spatial series of mean variance integrated towards the simulation period. The dotted vertical line represents the confidence level 95% while the green points represent the locations where the time variability will be analyzed.

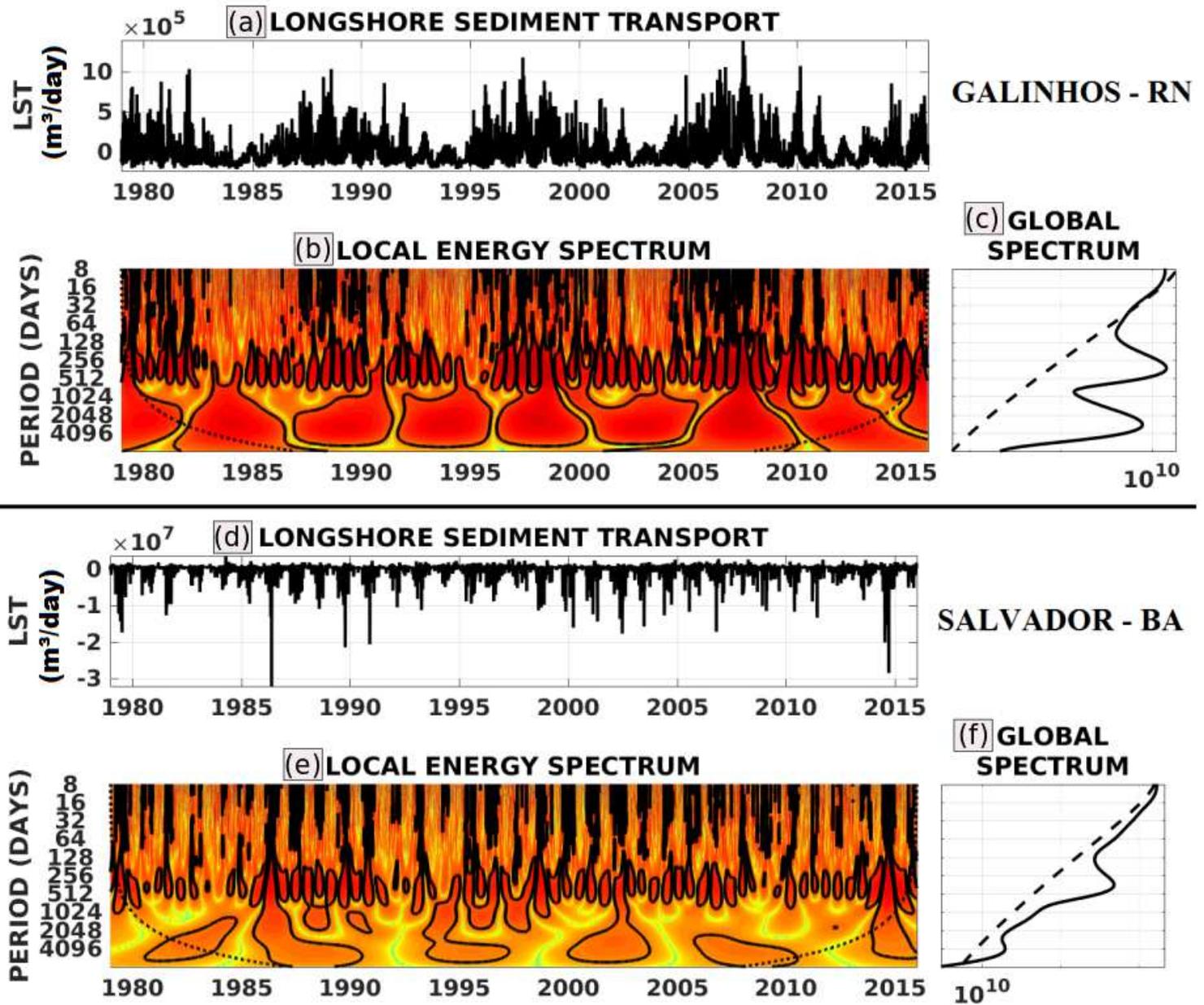


Figure 5

(a) and (d) Analysis of the Wavelet Method represented by the time series of longshore sediment transport in Galinhos - Rio Grande do Norte and Salvador - Bahia. (b) and (e) The local energy spectrum, and the black outlines represent the confidence level of 95% and the black dotted line represents the cone of influence. (c) and (f) The overall energy spectrum, and the black dotted line indicates the level of 95% confidence.

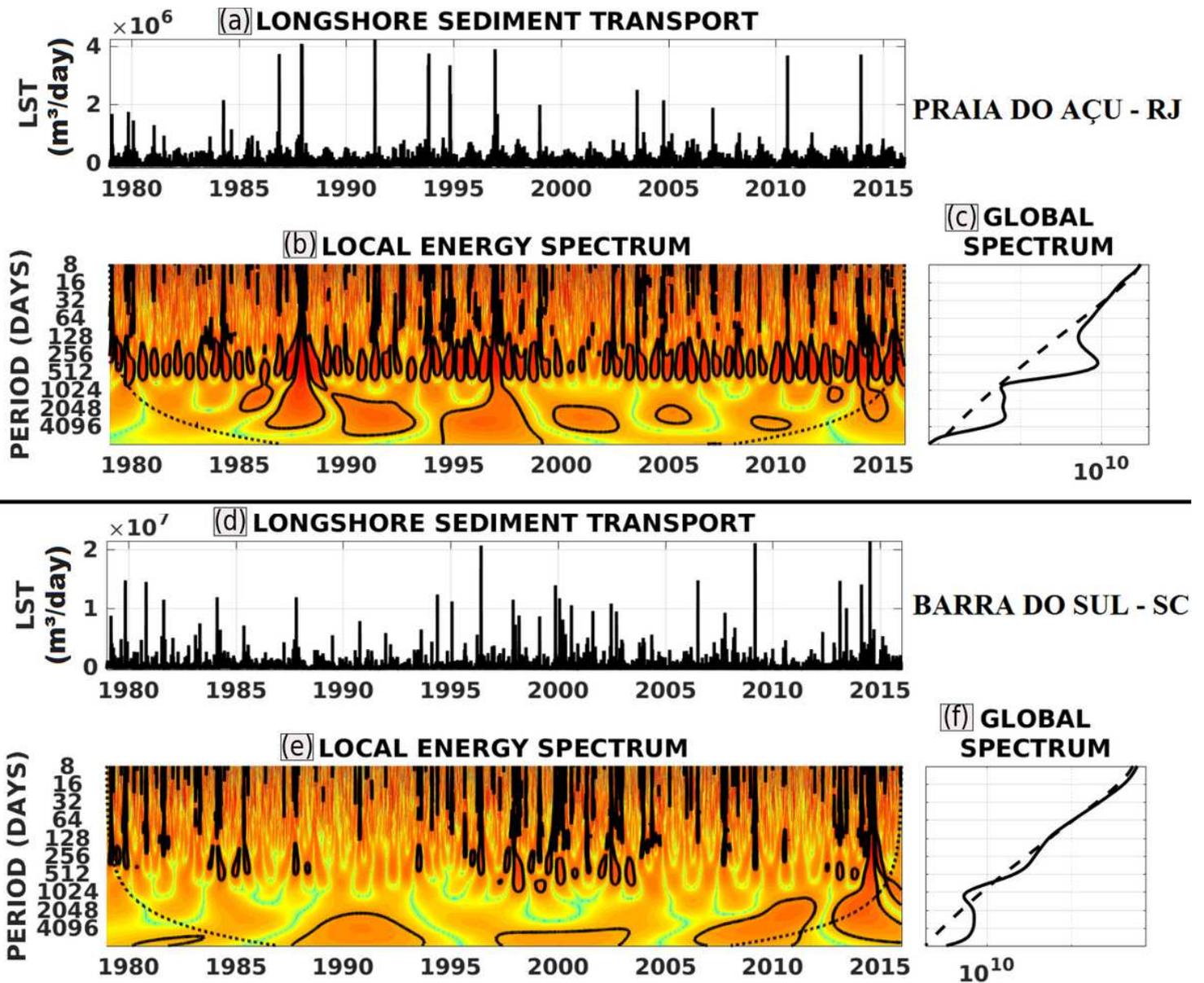


Figure 6

(a) and (d) Analysis of the Wavelet Method represented by the time series of longshore sediment transport in Praia do Açu - Rio de Janeiro and Balneário Barra do Sul - Santa Catarina. (b) and (e) The local energy spectrum, and the black outlines represent the confidence level of 95% and the black dotted line represents the cone of influence. (c) and (f) The overall energy spectrum, and the black dotted line indicates the level of 95% confidence.